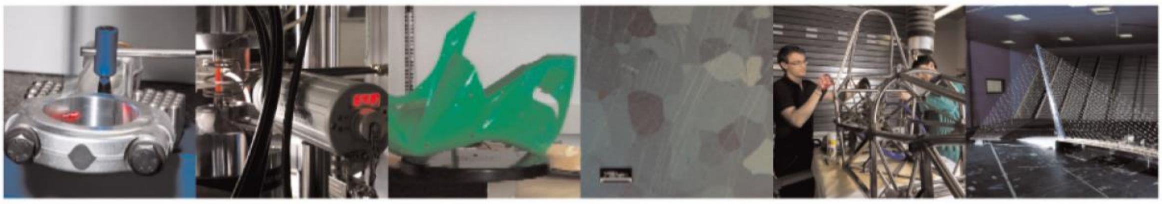

A comprehensive review of extrusion-based additive manufacturing processes for rapid production of metallic and ceramic parts

Rane, K.; Strano, M.

This is a post-peer-review, pre-copyedit version of an article published in ADVANCES IN MANUFACTURING. The final authenticated version is available online at: http://dx.doi.org/10.1007/s40436-019-00253-6]

A Comprehensive review of extrusion based additive manufacturing processes for rapid production of metallic and ceramic parts

Kedarnath Rane*, Matteo Strano

Dipartimento di Meccanica, Politecnico di Milano, Via La Masa 1, Milan, Italy

** Corresponding author. Tel: +39-0223998534, E-mail: kedarnath.rane@polimi.it*

Abstract

An extrusion based additive manufacturing (EAM) technique, recently became competitive for the rapid production of metals and ceramics components. This is made possible by extruding the metal or ceramic material in solid powder form, mixed with a binder, i.e. an expendable viscous fluid, which is removed from the part after 3D printing. The strength of these technologies relies on the large design freedom allowed by and by the cost efficiency advantage vs. alternative metal additive manufacturing processes based on high energy beams, e.g. laser/electron beam.

EAM of metals and ceramics is not yet widespread, and the published scientific and technical literature is rapidly growing, but still less extensive than the literature on FDM of plastics or SLM of metals. This paper aims at filling this gap. Fused Deposition Modeling (FDM) and Powder Injection Molding (PIM) are identified as preceding or enabling technologies for EAM.

This paper systematically reviews all the aspects of feedstock extrusion-based AM processes used for production of complex shaped parts. Then, the unique characteristics and advantages of the process are discussed, with respect to materials and process steps. The key process parameters are explained to illustrate the suitability of the process for diverse domains of applications.

Keywords: feedstock extrusion, rapid production, complex shaped metallic, ceramic parts

Nomenclature

Acronyms		Units	
PIM/ MIM	: Powder/ Metal Injection Molding	Kg	: kilogram
AM	: Additive Manufacturing	µm	: micrometres
FDM	: Fused Deposition Modelling	mm	: millimetres
EAM	: Extrusion based Additive Manufacturing	m	: metres
CAD	: Computer Aided Design	min	: minutes
AMF	: Additive Manufacturing File	s	: seconds

DED	: Directed Energy Deposition
DMLS	: Direct metal laser sintering
SSMED	: Semi-solid metal extrusion and deposition
DOD	: Drop on Demand
FEF	: Freeze-Form Extrusion Fabrication
SHS	: Selective heat sintering
SLM	: Selective laser melting
EBM	: Electron beam melting
PVB	: Polyvinyl butyral
PEG	: Polyethylene glycol
PW	: Paraffin Wax
HDPE	: High-density polyethylene
PP	: Polypropylene
PS	: Polystyrene
PEG	: Polyethylene glycol
PMMA	: Polymethyl methacrylate
PLC	: Programed Logic Control
CNC	: Computerized Numerical Control

1. Introduction

The term Additive Manufacturing (AM) was introduced in the '90s to describe a technology for manufacturing 3D components by creating layers. According to the standard ASTM International [1], AM is "a process of joining materials to make objects from 3D model data, usually layer by layer, as opposed to subtractive manufacturing methodologies, such as traditional machining".

These manufacturing technologies are attractive and prosperous in terms of rapid production of complex shaped objects of diverse materials, where complexity is obtained at competitive costs. AM is also resource-efficient because the parts are built by growing layers of a component from CAD data, with very little scrap or waste rate. The conventional shaping operations for the complexly shaped polymer, metal, and ceramic parts require the deployment of molds/dies to constrain the material to a specific shape. On the contrary, the AM processes can be seen as a nearly die-less shaping technique.

A broad classification of AM techniques is given by the abovementioned ASTM standard, according to the deposition and solidification methods. Among these techniques, AM by material extrusion is the most cost-efficient and widely diffused technology for a wide variety of applications. Focusing the analysis to metals and engineering ceramics, the most extensive R&D and commercial development of AM technology has been addressed towards powder bed fusion and direct energy deposition technologies [2] [3]. The use of extrusion-based AM techniques are much less used for metallic materials, but they are increasingly being used for building polymeric 3D parts.

Some relevant papers on extrusion based AM techniques have recently reviewed. In years 2014 and 2015, several authors published reviews of melt extrusion-based AM processes, e.g. [4] [5]. They focused mostly on the FDM process where a filament of polymeric material is used as the feedstock and extruded through a heated printing head. On the other hand, all available reviews that cover the AM of metals [3] [6] and technical ceramics [2] [7] do not pay attention to extrusion based techniques. Gonzalez-Gutierrez et. al [113] recently summarized the material extrusion process involving highly-filled polymers without considering the competence of extrusion systems like MIM for mass production and applicability in the diverse fields of interests as the similarities of MIM and EAM are not demonstrated. The scientific literature about extrusion AM of metals and ceramic is growing, but, to the authors' knowledge, no systematic review of this exciting and growing field is yet available. This paper aims to fill this gap.

The paper is organized as follows: in the following section 2, the main AM technologies for metals are briefly listed and described. In Section 3, the Powder Injection Molding (PIM) process is also briefly introduced, because it is a powder metallurgy process, that uses similar materials to extrusion based AM. The existing associated processes to extrusion of metal/ceramic feedstock are discussed in Section 4, namely freeform extrusion of liquid metals, deposition of slurries, filament and pellet based FDM processes. Section 5 illustrates the underlying technique, commercial systems, and materials used in feedstock extrusion based AM of metallic and ceramic parts. Quality assessment techniques for products processed by EAM is briefly explained in section 6 whereas current and prospective applicability of EAM in the aerospace, automotive, biomedical, and energy fields are discussed in Section 7. Recent progress and research needs of this AM technology also presented in this section.

2. Powder based AM processes for metals and ceramics

The most typical AM extrusion process is Fused Deposition Modeling (FDM), commonly used for plastics. The material in the form of a rod or wire is pulled through a pipe, heated up in a nozzle to ease flow during extrusion and gets layer-wise deposited. Other variants have been developed, suitable for metals or ceramics, which require mixing of a solid powder in a slurry or with a binder that melts during extrusion. These variants are the main subject of this review paper because they are generally neglected even by recent review papers on AM [8].

The increasing interest and technological advances of FDM allow to achieve superior dimensional control and properties of 3D printed objects [9]. The process starts with constructing a CAD model and preparing a digital surface model (.stl file). This model is processed by a specific software (eg. Slic3r), that divides the 3D model into slices. The thickness of layers is adjusted depending on the required part quality. The object is built by adopting hatching profile for infill structure and support structures for overhanging geometries. After finishing the build-up process for an object, the support structure is removed to get a final prototyped object [10], with a layered, textured surface. FDM finds its major applications in consumer goods because the process is well-known for processing of plastics. Nevertheless, recent developments allow its adaptability, thanks to improved accuracy [11], to suitability to extrude various feedstock materials [12] and integration with subsequent steps like debinding and sintering [13], for production of usable metal and ceramic parts.

Several techniques use powdered metals and ceramics to produce parts by additive manufacturing. All the AM techniques used for production of metallic and ceramic parts are briefed below.

a) Material Jetting: similar to a 2D ink jet printer where the material is jetted onto a stage. Drop on Demand (DOD) or continuous approach is used for jetting. The material gets hardened with the help of ultraviolet light, and the product is built layer by layer. Precision inkjet printing can be used for metals if the metal powder is mixed with a binder to form a slurry. Sintering eventually consolidates the printed green part. A material jetting DOD technique has been recently developed where liquid droplets of nanometric metal powder and a liquid binder are deposited [14].

b) Binder Jetting: In binder jetting, a liquid binder is used to bind the powder material which is stored in a powder bed. Layers of material are bonded by strategically jetting of drops of binders on powder bed to form an object [15].
c) Powder Bed Fusion: an energy beam is used to melt and then fuse powder material together, which is stored in a powder bed. Commonly used techniques use a laser beam as the energy source [16], examples are the direct metal laser sintering (DMLS), the selective laser melting (SLM) and the Selective Separation Sintering (SSS). SSS can fabricate high temperature ceramic and metallic parts at comparatively lower cost; it requires two kinds of powders, the base (B) powder which makes up the final part and a separator (S) powder. The 3D printed green part is later sintered in bulk [17]. Another typical source is the electron beam, used in Electron beam melting (EBM).
d) Directed Energy Deposition (DED): This process is widely used to repair or add extra material to existing parts. Various materials are deposited from any angle and melted by either an electron beam or a laser. DED can be done with polymers, metals, and ceramics but commonly used for metal, either in powder or wire form [18].
e) Extrusion based additive manufacturing (EAM): The multi-step process of EAM involves powder-binder mixture (called as feedstock) preparation, extrusion deposition of feedstock in the controlled manner to build 3D object and then post-processing (debinding and sintering) to obtained dense metallic/ceramic parts. Unlike binder jetting, the extrusion deposition phase of EAM process work similar to Fused Deposition Modeling of composite materials. The process is recently developed and may evolve further because of its simplicity, cost effectiveness and production speed [19, 20].

Products created using powder-based AM find continuously increasing applications in aerospace, medical, automotive, industrial, tooling and consumer goods [21]. Among the five classes of processes above mentioned, AM by extrusion promises to be the most cost-efficient option, because of comparably lower equipment cost and faster build-up rates.

3. Powder Injection Molding (PIM)

PIM is a manufacturing technology used for producing geometrically complex parts, to near net shape, with small dimensions and high quantities. Both MIM (Metal Injection Molding) and CIM (Ceramic Injection Molding) options are possible. Investment casting is the typical competing process to PIM [22]. There are four main steps in a PIM process: i) feedstock preparation/mixing, ii) injection molding, iii) debinding, iv) sintering. The feedstock material is a mixture of powder and binder; it is prepared in a special type of mixer, homogenized in an extruder and pelletized for uniform feeding to the injection system. In the injection molding step, a "green" part is formed by injecting feedstock into the mold. The binders are then removed in the debinding step, which is made of two operations: solvent debinding and thermal debinding. Solvent debinding is implemented for removal of sacrificial binder constituents (generally low molecular weight waxes), whereas backbone binder is removed during thermal debinding. The debinded part, called "brown", is then sintered to achieve desired densification and sintered properties [23]. PIM processes are suitable for applications in automotive, orthodontics, micro and regular sized electro-mechanical, and precision devices [24].

4. Variants of Extrusion Techniques ~~and Injection~~ for Freeform Fabrication

According to the above-mentioned ASTM classification of process families, AM technologies that work by deposition of the work material can be defined as based on extrusion or on jetting. In extrusion, a continuous filament of solid, semi-solid or liquid material is extruded through a nozzle following a given path. The most intuitive way of creating a layered 3D metal part by deposition out of a continuous extrusion is trying to treat a metal alloy as polymer melts are treated in conventional FDM. If the metal is in a liquid or semi-solid form when pressed inside the extrusion nozzle, and if the metal can rapidly solidify soon after extrusion, the FDM process can be transformed and adapted for metal alloys. Some authors have worked on this concept, but in all available examples, the main limitation is the melting point: alloys with a low-temperature melting point can be, with special devices, 3D printed. This process is commonly termed as semi-solid metal extrusion and deposition (SSMED) because it utilizes the extrusion of a metallic filament (for alloys like Sn-15Pb, Pb-40Sn) in a semi-solid state (thixo-extrusion) to build the 3d part [25]. On the contrary, it is virtually impossible to extrude steels or ceramics. While some AM processes by material jetting of droplets are available which can deal with low melting points metals (e.g. aluminium, copper [26-30]), no EAM process is known that can deposit a filament of a pure metal alloy or ceramic. As follows, the available options are described.

4.1 Deposition of water-based slurries

The extrusion of slurries with low viscosity (usually below 10 Pa·s) with a large content of wet fraction has been proposed by several authors, since a long time, in the AM of ceramic parts. An important option is the so-called Robocasting technology, reviewed in [31]. Robocasting (sometimes also called ink-writing) is an extrusion fabrication technique used for dense ceramics and composites. It is based on the layer-wise deposition of loaded colloidal water slurries.

The feedstock material is nearly free of polymeric binder (less than 1%). The water volume fraction is typical > 30%, but more often in excess of 50%; the rest of the feedstock is made by ceramic powder. Recently, non-aqueous liquids, such as fatty acid-based suspensions, are being tested to formulate storable feedstocks [32]. A variant of the robocasting technique is Freeze-Form Extrusion Fabrication (FEF), where a suspension or colloidal gel is deposited and frozen onto a cooled substrate [33].

After deposition, the slurry must be dried and completely sintered; usually, the whole post-treatment cycle requires less than 24 hours. Sintering conditions depend on the powder material; it is generally performed in air, at temperatures that obviously depend on the specific material, generally higher than 1100°C [34].

Relevant and recent applications of robocasting are especially the production of bio-mimetic or bio-compatible scaffolds. As an example, a method is proposed for producing titanium-fiber reinforced 13–93 bioactive glass scaffold, which can be used for bone repairing implants [35]. Dental implants are also an important application [36]. Very fine lattice structures can be produced, as shown in Figure 1, because of the low viscosity of the slurry; in fact, extrusion nozzles as small as 100 μm can be used [7]. As an FDM variant, robocasting is attractive for in-hospital 3D printing due to its simplicity and low-cost. In fact, many robocasting 3D printers under 10,000 € have become commercially available [37].

Some applications, not many indeed, can be found for the extrusion of slurries loaded with metal rather than ceramic particles. As an example, in a slurry made of Ti6Al4V powder (66 vol %), mixed with an aqueous solution of methylcellulose and stearic acid (34 vol %) was extruded with a syringe, to create biocompatible scaffolds for growing bone tissues [38].

4.2 FDM of advanced ceramics and metals starting from pastes or suspensions

The use of water-based slurries was replaced, by some authors, with polymeric pastes or suspensions with relatively low viscosity, ranging from 10 to 100 Pa·s. An early attempt was proposed with a paste made of PMMA or PVC binders instead of water mixed with aluminum powder [39]. The low solid fraction (max 70% aluminum by weight) allowed injection with a simple syringe. In (Grida et al. 2003) a suspension of 55 vol.% zirconia in a thermoplastic wax-based vehicle was extruded through a range of fine nozzles with diameters from 76 to 510 mm. The low viscosity of the suspension allowed injection with a syringe system, pressurized with a nitrogen gas at a constant pressure of 350 kPa [40].

In (Bellini et al., 2005) a heated screw extruder, loaded with pellets of lead zirconate titanate (PZT) ceramic powder mixed at 55 vol. % solid loading in a thermoplastic binder was used for the fabrication of simple structures [41].

In (Lu et al., 2008) an alumina powder at 60 vol. % solid loading was mixed with a thermoplastic polyvinyl butyral (PVB) and with polyethylene glycol (PEG) solvent based mixture. The resulting paste was pre-filled in a stainless steel syringe and injected by a micro extruder (50,000 steps/rev micro-stepper motor) [42]. The schematic diagram of a paste extrusion system is shown in Figure 2.

The thermoplastic binders used in these mixtures must be removed during long and critical post-processing operations of debinding and sintering. Besides, 3D printed parts made from solvent-based pastes not only need debinding and sintering, but they also require, before debinding, a few hours for drying, i.e., for solvent evaporation. Syringe-based systems did not allow to inject pastes with high solid loading (and high viscosity), hence the further difficulty of the debinding phase, in comparison with water-based slurries. Unlike premixed feedstock, pastes are not a commercial product and require long and critical preparation steps [43, 44].

4.3 FDM of advanced ceramics and metals starting from filaments or rods of binder/powder feedstock

Fused Deposition Modeling (FDM, sometimes referred to as Fused Deposition Molding) is by far the simplest, most cost-efficient and consequently diffused extrusion based AM technology worldwide for engineering, consumer, and architectural applications. As stated in the Introduction, it is mostly used for polymers, but its variants can be used for metal and ceramics, too. These process variants are described as follows. In conventional FDM approaches, a filament of polymeric material is extruded through a heated printing head. In order to be used for advanced ceramics and metals, the filament can be previously prepared as a mixture of polymeric binder and either ceramic or metal powder loading. Unlike robocasting mixtures, where the binder percentage is negligible, in FDM of filaments, the binder percentage is remarkable; in works pioneered by Rutgers University, the volume percentage powder loading of ceramic or metal did not exceed 50% -60% [45, 46]. In the year 2000, mounted a high-pressure extrusion head onto a conventional Stratasys FDM machine, allowing the 3D printing of green ceramic feedrods [47]. In some applications, e.g. for producing polymer-ceramic composite scaffold or when the desired 3d printed part is a metal/polymer composite, the debinding operations are not required [48].

In Figure 3, an image is shown of a system designed for extrusion of filaments. This technology did not have significant diffusion during later years, probably because of the many problems connected with extruding a stiff filament made of a pre-mixed and pre-extruded polymer/powder mixture [47]. Furthermore, it is difficult to prevent buckling of the filament and other problems when the viscosity of the melt increases and this limits the powder volume fraction that can be used. High powder loading should be preferred because this facilitates the success and quality of the debinding and sintering processes.

4.4 3D printing of advanced ceramics and metals starting from pellets or granules

Due to the inherent limitations of FDM processes that use filaments or paste as the raw material (described in the previous sub-sections) an alternative type of feedstock has been recently proposed by some authors, made of pellets or granules which have been produced as blends of polymeric binder and high solid powder loading. Replacing the syringe injections systems used in Robocasting and similar methods with high-pressure extruders was the technological innovation which enabled the use of highly dense and viscous thermoplastic-based feedstock, with viscosity values above 100 Pa·s. At the same time, the use of pellets or granules instead of filaments or pastes has allowed increasing the availability of material combinations and to use commercial injection molding materials.

A research group of Shenzhen University initially proposed to implement an FDM process using the same feedstock material mix in use for powder injection molding machines [51]. They used a stainless steel powder and thermoplastic paraffin wax-based binder, extruded through a screw extruder and they started studying the material properties of the green and sintered extruded filaments. In a technical magazine, a demonstrative robotic system was described, developed at the Lockheed Martin and Oak Ridge National Lab (ORNL) that deposits high-performance engineered thermoplastics, potentially able to work with pellets of powder/binder mixtures [52]. However, no scientific information was available. Some years later, this idea was further developed at Politecnico di Milano [53], where a fully functional AM machine was built, combining a small electric injection molding unit with a parallel kinematics (linear delta) table (see Figure 4). This system can extrude a mixture with as much as 70% solid loading by volume. Organic, water-soluble binder systems are preferred in these first attempts. The mechanical properties of the deposited, debinded and sintered parts are comparable to the homogenous wrought alloys [54]. Very recently, commercial machines which are capable of implementing the FDM of pellets loaded with metal or ceramic powders are becoming available, such as the Arburg Freeformer [55] or the Desktop Metal Studio System [56].

5. Description of Extrusion based additive manufacturing (EAM) process

The process of EAM is divided into three distinct groups of operations, (i) feedstock preparation, (ii) deposition/3D printing and (iii) post treatments. The schematic representation of the process shown in Figure 5 gives a clear understanding of the essential process steps. The starting material (the feedstock) is the homogeneous mixture of metal/ceramic powder and binder constituents. The mixture is prepared using compounding equipment and through an extruder and pelletizer for homogenization and easily feeding to extrusion-based AM (EAM) machine [57]. 3D deposition is accomplished by synchronizing fed of feedstock material with moving table or extrusion head.

The obtained shape (green state) after freeform deposition does not represent a final part because of alterations in part characteristics during subsequent steps. Post treatments like debinding for removal of binder constituents, sintering for powder consolidation to near full density and optional finishing are used to obtain the final usable part. In the following subsections, the operations and the components listed in Figure 5 are discussed.

5.1 Suitable Materials

The starting material for the process, usually termed feedstock, is a homogeneous mixture of metal or ceramic powder and multi-component binder. Metal and ceramic powders are used as a solid loading for preparing the feedstock. Powders are produced by several methods, particularly gas atomization, water atomization, milling, oxide reduction, precipitation. Both gas and water atomized powders are known to provide spherical particle morphology. Gas atomized powders have more uniform shape and size distribution over water atomized powders, but the associated cost is higher. The tradeoff between attributes mentioned above of powder is necessary to balance the powder characteristics so that the resulted feedstock should be able to facilitate free flow during extrusion, stability during debinding and densification during sintering [58].

Suitability of powder materials for an AM process is decided using powder characteristics such as mean particle size, particle size distribution, particle shape, specific surface area, and chemical composition. Moreover, to select an appropriate powder for extrusion-based AM process, few more characteristics about solid loading, inter-particulate friction, flow during extrusion, shape stability during debinding and sintering also plays a crucial role. The formulation of feedstock is the first important step in the process because of (a) the formulation interacts with characteristics mentioned above and decides the final quality of parts and (b) powder content in formulation makes up the major volume of the final sintered parts. Green parts typically have about 45 to 75 volume percent of powder loading [58].

The deposition process requires particles that are smaller than 20 µm. Fine particles are preferable for EAM process as the allied process PIM uses fine particle size powders to facilitate flow during extrusion/injection and to improve sinterability. However, the finer are bonded to form larger diameter chunks. The spherical shape of powder particles is preferable which reduces internal-particulate friction and avoids particle interlocking to achieve better flow for isometric part structure. On the contrary, irregular particle shape increases mechanical interlocking and sintered density. Multimodal particle distribution offers the benefit of higher possible solid loading which subsequently results in lower sintering distortion and high sintered density. The powder influences sinterability, surface finish, and minimum feature size, strength of part, etc. characteristics.

ASTM F3049-14 standard introduces the technique to characterize powder material used in powder-based AM processes [59]. For determination of powder particle size, sieving test is not applicable because powder particles smaller than 45µm are required and sieve opening from 45 to 1000 µm are used to measure particles. The use of light scattering is suitable for powder used in such EAM process since this technique is suitable for 0.4 µm to 2 mm particle range. Image analysis method is also applicable for measuring size distribution. There is no qualitative definition for many powder shapes. However, morphology can be determined by light scattering and image analysis methods. Inert gas fusion, X-ray fluorescence or optical emission spectroscopy can be used for chemical analysis of powders. Tap and skeletal density (measured by helium or nitrogen pycnometer) are also determined for specifying powders in AM [59].

The so-called binder system is a multi-constituent material used to shape and support of the powdered part structure. One of the main components is termed backbone, which supports and maintains the shape of the molded part until the last stages of debinding. High and low-density polyethylene (HDPE and LDPE), ethylene vinyl acetate (EVA), polyethylene (PE), polypropylene (PP), polystyrene (PS), polymethyl methacrylate (PMMA) are among the widely used backbone binder constituents [60].

The second component, sacrificial binder (usually paraffin or carnauba wax, or agarose), is required in a similar proportion to the backbone to induce flowability during extrusion. Such component should be easily removed in early stages of debinding (solvent debinding), leaving open pores that alows the gaseous products of the remaining backbone binder to diffuse out of the structure. The low-melting temperature component has an important role in the process, but the mechanical integrity of the final product is reduced as its proportion increase after a certain limit [61].

Brief information about metallic/ceramic powders and related binders used in various AM studies are summarized in Table 1. Variety of feedstock materials used in extrusion-based AM is covered. Among metals, Copper, Stainless Steel (17-4PH, 304L, 316L), Inconel 718, Tool steel (M2, SKH10), Titanium (Ti6Al4V) are the most widely used. Ceramic materials like Alumina, Zirconia, Cemented carbide (WC-8Co, WC-10Co), Silicon carbide, Silicon nitride are also extensively used in multiple areas of applications. Metal and ceramic powder loading is ranging from 60 to 80 vol. %. Binder system as discussed above contains either petroleum based (like paraffin wax, HDPE, etc.) binders or water-soluble binders (like methylcellulose, polyethylene glycol, etc.). Due to process similarities, the feedstock used in powder injection molding can also be adopted for extrusion-based AM. In Table 2, selected feedstock formulations (used in powder injection molding) are presented to appreciate compatibility of a process for a diverse range of materials and applications. However the solid loading and binder constituents may be further optimized when tailored particle size distribution (for high packing density and low cost), different particle shapes, minimized explosion and toxic hazards, clean particle surface with the binder are considered in EAM process [19, 62].

Important selection criteria for binder system is the choice of debinding mechanism. For processing of ceramics and noncorrosive metals, water soluble binder system (e.g. with wax and polyethylene glycol (PEG)) is simpler and preferable. However, organic binders are versatile, costlier for debinding but lead little residues after debinding [61].

Additives and surfactants are the supplementary constituents (quantity usually less than 2 wt. %). Surfactants like stearic acid act as a lubricant during deposition to reduce inter-particulate friction; they are commonly added to powders to form a thin outer layer on a particle surface, which leads to a more homogeneous packing structure. However, these short molecules/surfactants are causing bubbles and cracks when added in excess (more than 5 wt. %) [26].

5.2 Feedstock Preparation

The feedstock is prepared by compounding binder constituents with fine metallic or ceramic powders. Tumbler mixer (double cone mixers) are widely used for the dry blending or mixing of powders. During compounding, the surface of each particle is coated with binder. High-shear mixers (planetary or z blade, as shown in Figure 6) and roll mills are used for batch compounding. Screw extruders and shear rolls are commonly used for continuous compounding [80].

The appropriate volume of binder for a given powder depends on the characteristics of powders. The powder content in feedstock usually ranges from 50 to 65% by volume. The powder content (less than 50 vol.%) hinders the sintering ability of the feedstock and lowers the final density of the part. However, the extrusion step is facilitated by the lower viscosity of the feedstock [76]. Feedstock material is commercially available in the shape of pellets for easy handling.

The melt flow characteristics of feedstock is studied using rheological tests by varying temperature and strain rate. The optimum extrusion process parameters governs the steady flow feedstock as too low extrusion temperature and extrusion speed require a very high extrusion pressure. On the contrary, at very high extrusion temperature, the binder start degrading inside the extrusion chamber and cause a discontinuity in the feedstock flow [81, 82].

5.3 Machines for extrusion based additive manufacturing

An extrusion system commonly used in FDM, is shown in Figure 7 (a). A pinch feed mechanism is used to feed spooled filament of a feedstock to the liquefier for melting and controlled deposition. The incoming solid filament acts as a plunger to push and extrude the molten feedstock through the nozzle. This system has limited applications due to availability and manufacturability of filaments of feedstock materials. Secondly, the filament feeding mechanisms in FDM limit the use of low viscosity materials because of buckling and back-flow induced flow instability [83]. To avoid these challenges and to improve the reliability of the continuous printing, screw-based and piston-based extrusion systems are developed. The most common method for extrusion are syringe/piston based extrusion as shown in Figure 7 (b) and screw-based extrusion as shown in Figure 7 (c). These systems require hydraulic or electric drives to push the molten feedstock. The extrusion unit consists of a plunger or a screw, a heating system and a nozzle. The screw-based system increases the extrusion pressure and reproducibility of dimensions [84]. The molten feedstock is extruded and free-form structure is created by control movement of either table or extruder. The required pressure (about 2 to 10 MPa) in the extruder for this type of freeform fabrication is significantly lower than that required in MIM to fill the mold cavity (about 55 to 60 MPa for 60 vol.% powder loading) [85]. The heating system brings the material to required extrusion temperature. The nozzle is the duct for depositing the molten feedstock at a controlled velocity and flow rate.

Machine design considerations are necessary while designing machine architecture and also while optimizing machine dimensions. As far as the printing machine kinematics is concerned, most published examples on EAM of metal/ceramic feedstock use the typical FDM configuration, with a stationary build platform and an extrusion head moving in the Cartesian coordinates X-Y-Z whereas recently developed delta machines use a more complex control system due to their trajectories generation. Rapid speed and building capacity, higher production volume, less inertia of the extrusion assembly are the reported merits of delta machines for 3D printing [86].

In order to achieve complex trajectory generations a special tool path planning is required. This further improves the printing performance in terms of better surface finish, dimensional accuracy and minimizes the build-up time. Direction parallel (DP) tool path with constant feed rate conforms the uniform material deposition [87]. Whereas change of material flow improves the deposition in parabolic segments. A curvilinear abscissa velocity control is used for linear and parabolic trajectories to attain a better printing velocities. The control system is based on either a Programed Logic Control (PLC) and a motion unit or a Computerized Numerical Control (CNC). Combination of PLC and motion unit allows customizing the trajectory of the system according to different needs however the associated cost is significantly higher.

A recently developed extrusion based system uses a parallel kinematic and controlled acceleration of actuators for generating path trajectories of the work table. Three translational and two rotational degrees of freedoms allow efficient deposition of material on given trajectories. A robot (as shown in Figure 8) having 5 degrees of freedom (DOF) was developed for movement of worktable for extrusion-based 3D printing [89-91]. Kinematic conations with 5 DOF allow to reduce significantly the typical staircase effect on the surface of 3D printed parts.

The ratio between extrusion velocity and x–y movement of the nozzle should be maintained at unity to obtain the quasi-constant diameter of extruded wire for better geometrical accuracy and interlayer bonding [27]. Critical nozzle height ($h_c = \frac{D_n \times v_d}{v_n}$ where v_d is the extrusion rate (cm^3/s), D_n is the diameter of nozzle (mm) and v_n is the nozzle moving speed (mm/s)) is the quality control parameter. Height of nozzle from platform or previous layer should be equal to critical nozzle height for geometric accuracy of fabricated part [36]. The extrusion temperature is another critical parameter which defines the flow of feedstock. Melt viscosity determined from rheological tests are used to conform the uniform flow and minimal swelling during deposition. The desired viscosity of the feedstock is achieved by an optimal combination of extrusion rate and extrusion temperature [81]. The temperature of the deposition plate also needs to be set well to avoid part warpage and to improve layer adhesion to the plate for part stability [20, 92]. Among the parameters concerning deposition strategy are:

(a) Perimeter which enhance the surface finish of printed parts, generally, the perimeter consists of 1 or 2 roads before filling the rest in with a standardized pattern infill.
(b) Infill defines the internal structure of the part. The infill can be created using different strategies, by managing patterns and percentage of material fill.
(c) Hatch Spacing is the distance between the centers of two parallel roads. This parameter further explains the infill and the density of the overall part [82,92].

5.4 Debinding and Sintering

Before sintering, the binder is removed from the green part. The debinded parts are called "brown". The debinding is the most expensive and time-consuming stage. Two primary methods are applied for binder removal: solvent and thermal debinding. First, the component is immersed in a solvent that dissolves some binder constituents leaving some open pores to facilitate further removal of backbone binder during thermal debinding [93].

Wax based systems are used in commercial MIM production because waxes dissolves easily and completely in petroleum based solvents. Whereas water-soluble binder system works relatively slower as solvent in this case is just normal water. The use of CO_2 in supercritical conditions as a solvent was studied by [94] for accelerated removal of binders like PEG. Supercritical debinding can be implemented for diminution of time of debinding without disturbing the integrity of parts. The handling of parts is crucial after solvent debinding [94].

The thermal debinding is a relatively easier step as the binder is removed by degradation, evaporation, or liquid extraction at temperatures of about 200 to 600 °C. Catalytic debinding systems utilizes a combination of thermal and solvent debinding mechanisms wherein the polymer chains of the primary binder were broken back into its monomer form with the help of a catalyst. The catalytic debinding is based on solid-to-vapor catalytic degradation; this makes removal of binder faster and improves the strength of brown parts, which is critical in the handling operations [95].

The sintering step is the last step which is often directly incorporated after thermal debinding. Sintering provides the inter-particle bonding which leads to densification. Depending on the material, brown parts are sintered and results in high sintered density ranging from 95% to 99.5% of theoretical full density. Sintering temperature in the range of 1120 to 1350^{o}C and sintering time of 30 to 120 minutes are standard for iron and steels. Commercial systems (desktop metal, etc.) uses combined resistance based heating and microwave heating to expedite the diffusion of metal particles for densification and produce a highly dense sintered metal parts. The part shrinks by 12 to 18% during sintering phase of EAM process. The sintered parts from EAM and MIM have comparable characteristics and said to have superior mechanical properties than the conventional pressed and sintered parts. This is because both processes require smaller particle sizes of powder which improve the sinterability of part and impart higher sintered density and mechanical strength

[96]. Industrial units have a continuous debinding and sintering process to enable the economical production of parts. Parts are placed on ceramic trays in the sintering furnace for batch type production units.

The properties and dimensional characteristics of sintered components can be further improved by many of the standard finishing processes that are applicable to wrought metals and/or PIM components. However, the surface quality of AM components can be improved by means of machining operations performed already at the green state, before debinding [97]. With increasing applications of EAM, the use of different materials and the complexity of the produced components get increased. Recent developments in hybrid manufacturing machines allows to obtain the usable parts with improved dimensional and surface characteristics even by intermediate machining operations during EAM process [98].

6. Quality assessment of products manufactured through EAM process

In extrusion-based AM process (similar to powder injection molding), after sintering a part has dimensions significantly different to those of the 3D printed (green) parts. Shrinkages and distortion during sintering achieve dimensional tolerances quite challenging. The shrinkage is due to the high-volume percentage of binder in green part (as much as 50%), and during sintering, a large shrinkage occurs. Therefore, it is essential to ensure that this shrinkage is controlled during the sintering process. In this regard, the process is competitive with other AM techniques only if the mixture/feedstock is homogeneous so that the shrinkage is uniform and isotropic.

For many of the engineering applications, the quality of prototypes is quantified regarding surface finish and dimensional stability. Specific standards for governing product characteristics of extrusion-based AM (EAM) are not available. Available guidelines from ASTM standards related to general AM processes can be useful for the new EAM process.

Guidelines given in ASTM F3091 suggest using both direct independent and direct dependent properties for quantification. It also specifies dimensional tolerances in the range of ±0.1 mm [99]. Mechanical properties of metallic parts made via AM are characterized according to the guidelines given in ASTM F3122-14. Deformation test (tension, compression, bending) referred to the corresponding general testing standards E8, E9 and E209 respectively. Fatigue properties are characterized at room temperature according to E466 standard. ASTM E606 describes testing using primary strain controlled fatigue with the magnitude of dependent inelastic strains [100].

The process parameter layer thickness is the most significant on the quality of FDM process. Road width and speed are also contributing significantly to surface roughness of parts. Moreover, the granulometry of the powder, rheological properties of the feedstock and the viscosity at the extrusion temperature are other essential qualities measures [73].

6.1 Mechanical and metallographic characteristics of EAM parts

A limited literature is available on specific properties of parts obtained from this process. Most of them discuss mechanical characteristics in terms of yield strength, flexural strength, and porosity. The strength of green part was investigated using tensile testing and compared through measurement of printed distance, layer thickness and distance of voids as shown in Figure 9. Green strength the copper specimen was reported in the range of 5 to 6 MPa. This study also demonstrated that influence of infill degree is significantly higher that layer thickness and orientation of deposition on green strength [54].

Ren et al. also reported the hardness and yield strength of sintered samples of extrusion-based 3D printed parts. These properties are reproduced in Table 3. It shows that mechanical strength of extrusion-based 3D printed parts are comparable with wrought copper and other additively manufactured copper parts [54].

Another study by Li et al. shows that the compressive strength of additively manufactured Ti_6Al_4V scaffolds increases with extrusion pressure (Figure 10 (a)) and decreases with increasing feeding speed (Figure 10 (b)). This is a direct consequence of porosity change. The porosity of scaffold was decreased with increasing pressure and decreasing feeding speed [38].

Effect of solid loading on flexural strength was investigated by Thomas et al. (presented in Figure 11). The flexural strength and flexural modulus are increased with the progressive addition of the Ti fiber. Volume fraction addition higher than 40 % of Ti fibers in the 13–93 glass paste caused clogged nozzle tips and hence not considered to be feasible for freeform extrusion fabrication [35].

Metallographic investigation of alumina part is shown in Figure 12. Microstructure shows grains are small (<5 µm) and equiaxed. No printing defects are observed when these alumina part were sintered at 1550°C for 2 hours [101].

6.2 Effect of process variables on the part characteristics

The EAM process utilizes sintering step wherein parts heat uniformly to just below their melting point to form fully dense parts without the residual stresses which are introduced in laser-based systems [56].

The effect of fluidity on the deposition of Ti6Al4V rod was studied by [38] for the manufacturing of scaffolds. During deposition of the rod, a lower viscosity of melt results in deformation of the deposited rod, and a higher viscosity of material causes a higher resistance against flowing and affect the quality of parts.

The powder concentration is an important factor which affects the viscosity of the melt, as reflected in Figure 13 where Ti6Al4V powder used as a solid loading for the production of scaffolds. Both too low and too high concentrations of powder have undesirable effects, respectively a gravity-induced flow after depositing (Figure 13 (A)) and little or no attachment between the layers (Figure 13 (C)) respectively. Melt with a 66 volume % concentration of powder shows a tradeoff for a good quality of parts (Figure 13 (B)).

Presence of humidity between 13 to 17% (as seen from Figure 14) was found to be optimum for the extrusion of alumina parts without deformation due self-weight and cracks. Addition of plasticizers (such as Zusoplast C28) in 1 to 3 wt% with 15% humidity improves the plasticity of alumina emulsions [68].

7. Current and prospective applications of EAM process

Intensive research and progress made in development and commercialization of additive technologies have broadened the application spectrum of these technologies. These processes are currently used by multiple industry subsectors, including aerospace automotive, electronics, and medical products. The EAM technologies can compete with the alternatives in terms of associated lower cost and comparatively higher production volume (build up rate) [102]. When net shaped parts are needed in smaller quantities, the developed technology also provides an alternative to mold making which relates to the major cost of PIM process. The developed simulation tools can significantly help to improve process capabilities by to minimizing the process errors for successful printing [103].

Here as follows, only a few examples of applications found in the literature are mentioned.

Biomedical applications. In [36], an artificial human teeth and crowns of Porcelain were fabricated via a Slurry Micro Extrusion (SME) process as shown in Figure 15. The prepared slurry with 40-45 vol. % solid loading is deposited with changeable 100-800 µm diameter nozzles. Isotropic shrinkage of the green teeth during sintering is about 25% when sintered at 950 ^{o}C for 24 hours. This requires to scale the CAD model to compensate the sintering shrinkage while printing the teeth (green state) and to improve dimensional accuracy after sintering. Likely defects such as rough surface, diameter variation, segregation of extruded parts can be addressed by proper mixing of feedstock, moisture removal, and prevention of overheating. Rapid prototypes and high-quality bone transplants in biocompatible metals are also possible because of material processing diversity of this process. Biomedical materials, like titanium alloys, pure titanium bone fixation Ti–6A1–4V artificial valve, stent, bone fixation Ti–6Al–7Nb, shape memory alloy NiTi catheters, zirconia porous implants are possibly processed by extrusion-based AM [32, 104].

Structural parts: Extrusion of feedstock having ceramic powder, particularly zirconia [105] and alumina [68] is possible for producing dense structural parts. Like other AM processes, the EAM enables the manufacture of complex cross-sectional areas. Thus manufacturing of complex shaped lightweight structures are possible [106].

Energy engineering parts: A 3d printed (green) part of an alumina impeller is shown in Figure 16 (a), prepared using extrusion of alumina mixed paste [101]. The performance of as-extruded fairly complex parts is not reported, but from the picture, no visible printing flaw is observed in part.

Other applications: The spectrum of potential applications of EAM for metals and ceramics in all engineering fields is too large to be completely reported. As a latest examples, in Figure 16, (c) sintered structural parts made of 17-4PH stainless steel [107, 108] and (d) shrinkage of a printed green part specimen in comparison to a sintered SS316 parts [62] are also incorporated. The sintered parts have sintered density, properties as comparable to the parts manufactured by MIM. A fully closed hollow metal components required in small quantities can be cost efficiently manufactured by EAM process for space and aviation application [108]. A novel multi-material transducer design (a multilayer ladder structure) was also demonstrated by [109] for possible application of EAM process, shown in Figure 17. In this structure, each layer contains roads of 250µm in diameter, deposited next to each other with a gap of 76µm in between. On the next layer, which is a different material, the roads are deposited with an angle of 90^{o} with respect to the layer. A stable, functional graded structure is evident from the sintered microstructure.

This review also highlights future directions that deserve exploration for the successful implementation of EAM based on early experimental results. Current efforts are focused extensively on (a) numerical analysis of process considering physical material phenomena and performance simulations govern through design and printing strategies, (b) development of process competence for improved part performance and (c) material availability and system integration to widespread application of EAM [102]. A brief assessment of EAM process with other mature AM techniques is given in Table 5 to identify the technological merits of the process. Binder jetting is the closest competing process that might prevent EAM to be established as a regular AM process in a broader manufacturing perspective. If considering the readiness of the process, it has already moved to preproduction and optimization and it is now approaching full rate production demonstration. Companies like Desktop Metal, Markforged, AIM3D already started production these machines for multiple domains of trades. Although we are still a long way from full-scale production of parts based on EAM process but the process will definitely receive increasing recognition and play an important role in future AM revolution.

8 Conclusions

The currently available literature on EAM and its closely related technologies have been reviewed. The steps of the process chain steps have been comprehensively illustrated. The process is versatile in terms of part materials as it uses metal/ceramic powder as a raw material and powders are available in various grades and characteristics. It can be considered a mold-less powder injection molding process. Mechanical properties, dimensional accuracy and surface roughness of sintered parts are different from the green parts. Extrusion settings directly influence these quality characteristics. They are also associated with material, debinding and sintering parameters. Maximum feature resolution of extrusion-based AM is determined from a minimum diameter of extrusion nozzle and maximum sintering shrinkage.

EAM for metals and ceramics has made considerable progress, and thanks to some very recent industrial player, might be on the verge of a commercial explosion, with a high potential thanks to the well-known advantage of FDM-like technologies in terms of build-up rate. As far as the scientific literature is concerned, little progress and technological advancement have been made by extrusion based AM technology regarding adaptability for real applications. The state of the art review unveils a need for improving performances in terms of overall prototyping time, accuracy, process control and cost-effectiveness.

References

[1] ISO/ASTM 52900:2015(E), Standard terminology for Additive Manufacturing, ASTM (2015).

[2] Deckers J., Vleugels J., Kruth J. P., Additive Manufacturing of Ceramics: A Review, J. Ceram. Sci. Tech. 05 (04) (2014), pp. 245-260.

[3] W. E. Frazier, Metal Additive Manufacturing: A Review, Journal of Materials Engineering and Performance 23 (6) (2014), pp. 1917–1928.

[4] B. N. Turner and S. A. Gold, A review of melt extrusion additive manufacturing processes: II. Materials, dimensional accuracy, and surface roughness, Rapid Prototyping Journal, 21(3) (2015), p. 250–261,.

[5] N. Turner, B. Strong and S. Gold, A review of melt extrusion additive manufacturing processes: I. Process design and modeling., Rapid Prototyping Journal, vol. 20, no. 3 (2014), p. 192–204,.

[6] K. P. Karunakaran, Alain Bernard, S. Suryakumar, Lucas Dembinski, Georges Taillandier, Rapid manufacturing of metallic objects, Rapid Prototyping Journal 18 (4) (2012), pp. 264-280,.

[7] J. A. Lewis, J. E. Smay, J. Stuecker and J. Cesarano, Direct ink writing of three-dimensional ceramic structures, Journal of the American Ceramic Society, vol. 89, no. 12 (2006), p. 3599–3609,.

[8] H. Bikas, P. Stavropoulos, and G. Chryssolouris, Additive manufacturing methods and modeling approaches: A critical review, Int. J. Adv. Manuf. Technology, 83 (1–4) (2016), pp. 389–405.

[9] Carneiro, O. S., A. F. Silva, Rui Gomes, Fused deposition modeling with polypropylene, Materials & Design 83 (2015), pp. 768-776.

[10] Tymrak, B. M., M. Kreiger, Joshua M. Pearce, Mechanical properties of components fabricated with open-source 3-D printers under realistic environmental conditions, Materials & Design 58 (2014), pp. 242-246.

[11] Bottini, A. Boschetto L., Accuracy prediction in fused deposition modeling, Int. J. Adv. Manuf. Technol., 73 (5–8) (2014), p. 913–928,.

[12] F. Ning, W. Cong, J. Qiu, J. Wei, and S. Wang, Additive manufacturing of carbon fiber reinforced thermoplastic composites using fused deposition modeling, Compos. Part B Eng (80) (2015), p. 369–378,.

[13] Brünler, R., Aibibu, D., Wöltje, M., Anthofer, A. M., & Cherif, C., In silico modeling of structural and porosity properties of additive manufactured implants for regenerative medicine, Materials Science and Engineering: C 76 (2017), p. 810–817.

[14] xjet3d.com, XJet's system, 06 09 2017. [Online].

[15] Miyanaji, H., Zhang, S., Lassell, A., Zandinejad, A., & Yang, L., Process development of porcelain ceramic material with binder jetting process for dental applications, JOM, 68(3) (2016), pp. 831-841,.

[16] W. E. King, A. T. Anderson, R. M. Ferencz, N. E. Hodge, C. Kamath, S. A. Khairallah, and A. M. Rubenchik, Laser powder bed fusion additive manufacturing of metals; physics, computational, and materials challenges, Appl. Phys. Rev 2 (4) (2015), p. 41304.

[17] Khoshnevis B., Zhang J., Selective Separation Sintering (SSS) A New Layer Based Additive Manufacturing Approach for Metals and Ceramics, in AIAA SPACE Conference and Exposition, (2015).

[18] D. Gallo, S. Biamino, P. Fino, and M. Lombardi, An Overview of Additive Manufacturing of Titanium Components by Directed Energy Deposition: Microstructure and Mechanical Properties, Appl. Sci. 7 (2017), p. 883.

[19] Rane, K., Cataldo, S., Parenti, P., Sbaglia, L., Mussi, V., Annoni, M., ... & Strano, M., Rapid production of hollow SS316 profiles by extrusion based additive manufacturing, In AIP Conference Proceedings, Vol. 1960, No. 1 (2018), pp.140014.

[20] Stavropoulos, P., & Foteinopoulos, P. Modelling of additive manufacturing processes: a review and classification. Manufacturing Review, 5 (2018), pp. 2-26.

[21] E. Atzeni, A. Salmi, Economics of additive manufacturing for end-usable metal parts, Int. J. Adv. Manuf. Technol. 62 (9–12) (2012), p. 1147–1155.

[22] R. M. German, PIM breaks the $1 bn barrier, Metal Powder Report 63 (3) (March 2008), pp. 8-10.

[23] A. Gonçalves, Metallic powder injection molding using low pressure, Journal of Materials Processing Technology 118 (1-3) (2001) pp. 193-198.

[24] German, R. M., Bose A., Injection Molding of Metals and Ceramics, New Jersey, USA: Metals Powder Industries Federation, Princeto, (1997).

[25] Jabbari, A., & Abrinia, K. Developing thixo-extrusion process for additive manufacturing of metals in semi-solid state. Journal of Manufacturing Processes, 35 (2018), pp. 664-671.

[26] Tseng, J.W. & Hsu, C.K., Cracking defect and porosity evolution during thermal debinding in ceramic injection molding, Ceramics International 25 (5) (1999), p. 461-466.

[27] Finke, S., & Feenstra, F. K., Solid freeform fabrication by extrusion and deposition of semi-solid alloys., Journal of Materials Science, 37(15) (2002), p. 3101–3106.

[28] Luo, J., Qi, L. H., Zhong, S. Y., Zhou, J. M., & Li, H. J., Printing solder droplets for micro devices packages using pneumatic drop-on-demand (DOD) technique, Journal of Materials Processing Technology, 212(10) (2012), p. 2066–2073.

[29] Zhong, S. Y., Qi, L. H., Luo, J., Zuo, H. S., Hou, X. H., & Li, H. J. Effect of process parameters on copper droplet ejecting by pneumatic drop-on-demand technology. Journal of materials processing technology, 214 (12) (2014), pp. 3089-3097.

[30] Zhang, D., Qi, L., Luo, J., Yi, H., & Hou, X. Direct fabrication of unsupported inclined aluminum pillars based on uniform micro droplets deposition. International Journal of Machine Tools and Manufacture, 116 (2017), pp. 18-24.

[31] J. Cesarano, A Review of Robocasting Technology, In MRS Proceedings 542 (1998), p. 133.

[32] Slots, C., Jensen, M. B., Ditzel, N., Hedegaard, M. A., Borg, S. W., Albrektsen, O., Simple additive manufacturing of an osteoconductive ceramic using suspension melt extrusion, Dental Materials 43, Issue 9 (2017), p. 198–208.

[33] N. Travitzky, A. Bonet, B. Dermeik, T. Fey, I. Filbert-Demut, L. Schlier, T., Additive manufacturing of ceramic-based materials, Adv. Eng. Mater. 16 (2014), pp. 729-754.

[34] M. Houmard, Q. Fu, M. Genet, E. Saiz, A.P. Tomsia, On the structural, mechanical, and biodegradation properties of HA/β-TCP robocast scaffolds, J. Biomed. Mater. Res. B. Appl. Biomater. 101 (2013), p. 1233–1242.

[35] Thomas, A., Kolan, K. C., Leu, M. C., & Hilmas, G. E., Freeform Extrusion Fabrication of Titanium Fiber Reinforced 13–93 Bioactive Glass Scaffolds, Journal of the Mechanical Behavior of Biomedical Materials 69 (2017), p. 153–162.

[36] Wang, J., Shaw, L. L., & Cameron, T. B., Solid freeform fabrication of permanent dental restorations via slurry micro-extrusion, Journal of the American Ceramic Society, 89(1) (2006), p. 346–349.

[37] I. 3. Bioprinter, 25 09 2017. [Online].

[38] Li, J. P., de Wijn, J. R., Van Blitterswijk, C. a, & de Groot, K., Porous Ti6Al4V scaffold directly fabricating by rapid prototyping: preparation and in vitro experiment, Biomaterials, 27(8) (2006), p. 1223–1235.

[39] Sercombe, T. B., Schaffer, G. B., & Lucia, Freeform fabrication of functional aluminium, Minerals and Materials, 4 (1999) p. 4245–4251.

[40] Grida, I., & Evans, J. R. G, Extrusion freeforming of ceramics through fine nozzles, Journal of the European Ceramic Society, 23(5) (2003), p. 629–635.

[41] Bellini, A., Shor, L., & Guceri, S. I, New developments in fused deposition modeling of ceramics, Rapid Prototyping Journal 11(4) (2005), p. 214–220.

[42] Lu, X., Lee, Y., Yang, S., Hao, Y., Ubic, R., Evans, J. R. G., & Parini, C. G., Fabrication of electromagnetic crystals by extrusion freeforming, Metamaterials 2(1) (2008), p. 36–44.

[43] Lu, X., Lee, Y., Yang, S., Hao, Y., Evans, J. R. G., & Parini, C. G., Fine lattice structures fabricated by extrusion freeforming: Process variables, Journal of Materials Processing Technology, 209(10) (2009), p. 4654–4661.

[44] Lu, X., Lee, Y., Yang, S., Hao, Y., Evans, J. R. G., & Parini, C. G., Solvent-based paste extrusion solid freeforming, Journal of the European Ceramic Society, 30(1) (2010), p. 1–10.

[45] Jafari, M. a., Han, W., Mohammadi, F., Safari, A., Danforth, S. C., & Langrana, N, A novel system for fused deposition of advanced multiple ceramics, Rapid Prototyping Journal (2000), p. 161–175.

[46] Wu, G., A. Langrana, N., Sadanji, R., & Danforth, S., Solid freeform fabrication of metal components using fused deposition of metals, Materials & Design, 23(1) (2002), p. 97–105.

[47] Vaidyanathan, R., Walish, J., Lombardi, J. L., Kasichainula, S., Calvert, P., & Cooper, K. C., The extrusion freeforming of functional ceramic prototypes, Jom, 52 (December 2000), p. 34–37.

[48] Kalita, S. J., Bose, S., Hosick, H. L., & Bandyopadhyay, A., Development of controlled porosity polymer-ceramic composite scaffolds via fused deposition modeling, Materials Science and Engineering: C, 23(5) (2003), p. 611–620.

[49] 3devo.com, 3devo.com/next-filament-extruder/, 13 10 2017. [Online].

[50] TheVirtualFoundry, www.thevirtualfoundry.com/showcase/m0mau80bklzxkr50voo7gkvrdqzs38, 12 10 2017. [Online].

[51] Li, J. B., Xie, Z. G., Zhang, X. H., Zeng, Q. G., & Liu, H. J., Study of Metal Powder Extrusion and Accumulating Rapid Prototyping, Key Engineering Materials 443 (2010), pp. 81-86.

[52] Holshouser, C., Newell, C., Palas, S., Love, L. J., Kunc, V., Lind, R. F, Peter, W. H., Out of bounds additive manufacturing, Advanced Materials and Processes, 171(3) (2013), pp. 15-27.

[53] Annoni, M., Giberti, H., & Strano, M., Feasibility Study of an Extrusion-based Direct Metal Additive Manufacturing Technique, in Manufacturing, 5, (2016).

[54] Ren, L., Zhou, X., Song, Z., Zhao, C., Liu, Q., Xue, J., & Li, X., Process Parameter Optimization of Extrusion-Based 3D Metal Printing Utilizing PW–LDPE–SA Binder System, Materials 10 (3) (2017), pp. 305, 1-16.

[55] Gaub, www.arburg.com/us/us/products-and-services/additive-manufacturing/freeformer-system, 2016. [Online]. [Accessed 2017 04 06].

[56] D. Rotman, Director, www.technologyreview.com/s/604088/the-3-d-printer-that-could-finally-change-manufacturing/. [Film] (2017).

[57] Tay, B.Y., Loh,N.H., Tor S.B., Ng F.L., Fu G. & Lu X.H., Characterisation of micro gears produced by micro powder injection moulding, Powder Technology 188 (3) (2009), pp. 179-182.

[58] K. K. Rane, P. P. Date, Rheological Investigation of MIM Feedstocks for Reducing Frictional Effects during Injection Moulding, Advanced Materials Research, 966-967 (2014), pp. 196-205.

[59] A. F3049-14, Standard Guide for Characterizing Properties of Metal Powders Used for Additive Manufacturing Processes, ASTM International, West Conshohocken, PA, (2014).

[60] Thomas-Vielma, P., Cervera, A., Levenfeld, B. & Várez, A., Production of alumina parts by powder injection molding with a binder system based on high density polyethylene, Journal of the European Ceramic Society 28 (4) (2008), pp. 763-771.

[61] Y. Kiyota.Patent US4867943 (1989).

[62] C. Burkhardt, P. Freigassner, O. Weber, P. Imgrund, S. Hampel, Fused Filament Fabrication (FFF) of 316L Green Parts for the MIM process, In Proceedings of theWorld PM2016 Congress & Exhibition, Hamburg, Germany, 9–13 October 2016; EPMA: Shrewsbury, UK (2016), pp. 1–7.

[63] Kang, H., Kitsomboonloha, R., Jang, J., & Subramanian, V., High-Performance Printed Transistors Realized Using Femtoliter Gravure-Printed Sub-10 μm Metallic Nanoparticle Patterns and Highly Uniform Polymer Dielectric and Semiconductor Layers, Advanced Materials, 24(22) (2012), pp. 3065-3069.

[64] Maleksaeedi, S., Eng, H., Wiria, F. E., Ha, T. M. H., & He, Z., Property enhancement of 3D-printed alumina ceramics using vacuum infiltration, Journal of Materials Processing Technology 214.7 (2014), pp. 1301-1306.

[65] Asadi-Eydivand, M., Solati-Hashjin, M., Farzad, A., & Osman, N. A. A, Effect of technical parameters on porous structure and strength of 3D printed calcium sulfate prototypes, Robotics and Computer-Integrated Manufacturing, 37 (2016), pp. 57-67.

[66] Gaytan, S. M., Cadena, M. A., Karim, H., Delfin, D., Lin, Y., Espalin, D., ... & Wicker, R. B., Fabrication of barium titanate by binder jetting additive manufacturing technology, Ceramics International, 41(5) (2015), pp. 6610-6619.

[67] Farzadi, A., Waran, V., Solati-Hashjin, M., Rahman, Z. A. A., Asadi, M., & Osman, N. A. A., Effect of layer printing delay on mechanical properties and dimensional accuracy of 3D printed porous prototypes in bone tissue engineering, Ceramics International, 41(7) (2015), pp. 8320-8330.

[68] Vitorino, N., Freitas, C., Ribeiro, M. J., Abrantes, J. C., & Frade, J. R., Extrusion of ceramic emulsions: Plastic behavior, Applied Clay Science, 101 (2014), pp. 315-319.

[69] T. Kono, A. Horata, and T. Kondo., Development of titanium and titanium alloy by metal injection molding process, J. Jpn. Soc. Powder Metallurgy 44 (1997), p. 985–992.

[70] Wen, G., Cao, P., Gabbitas, B., Zhang, D., & Edmonds, N., Development and design of binder systems for titanium metal injection molding: An overview, Metallurgical and Materials Transactions A, 44(3) (2013), pp. 1530-1547.

[71] Ahn, S., Park, S. J., Lee, S., Atre, S. V., & German, R. M., Effect of powders and binders on material properties and molding parameters in iron and stainless steel powder injection molding process, Powder Technology, 193(2) (2009), pp. 162-169.

[72] Levenfeld, B., Varez, A., & Torralba, J. M, Effect of residual carbon on the sintering process of M2 high speed steel parts obtained by a modified metal injection molding process," Metallurgical and Materials Transactions A, 33(6) (2002), pp. 1843-1851.

[73] Moballegh, L., Morshedian, J., & Esfandeh, M., Copper injection molding using a thermoplastic binder based on paraffin wax, Materials Letters, 59(22) (2005), pp. 2832-2837.

[74] Suri, P., Atre, S. V., German, R. M., & de Souza, J. P., Effect of mixing on the rheology and particle characteristics of tungsten-based powder injection molding feedstock, Materials Science and Engineering: A, 356(1) (2003), pp. 337-344.

[75] A. Bose, C. A. Schuh, Jay C. Tobia, N Tuncera, Ni. M. Mykulowycz, A. Preston, A. C. Barbati, Brian Kernan, M. A. Gibson, D. Krause, T. Brzezinski, J. Schroers, R. Fulop, J. S. Myerberg, M. Sowerbutts, Y.Chiang, A. J. Hart, E. M. Sachs, E. E. Lomeli, A. C. Lund, Traditional and additive manufacturing of a new Tungsten heavy alloy alternative, International Journal of Refractory Metals & Hard Materials 73 (2018), pp. 22–28.

[76] Merz, L., Rath, S., Piotter, V., Ruprecht, R., Ritzhaupt-Kleissl, J. & Haussel, J., Feedstock development for micro powder injection molding, Microsystem Technologies 8 (2-3) (2002), pp. 129-132.

[77] Samuel, I., & Lin, E, Near-net-shape forming of zirconia optical sleeves by ceramics injection molding, Ceramics international, 27(2) (2001), pp. 205-214.

[78] Yang, W. W., Yang, K. Y., & Hon, M. H., Effects of PEG molecular weights on rheological behavior of alumina injection molding feedstocks, Materials chemistry and physics, 78(2) (2003), pp. 416-424.

[79] S Ani, S. M., Muchtar, A., Muhamad, N., & Ghani, J. A., Binder removal via a two-stage debinding process for ceramic injection molding parts, Ceramics International, 40(2) (2014), pp. 2819-2824.

[80] B. Hausnerová, Powder injection moulding- An alternative processing method for automotive items, New Trends and Developments in Automotive System Engineering (2011), pp. 129-145.

[81] Peng, F., Vogt, B. D., & Cakmak, M. Complex flow and temperature history during melt extrusion in material extrusion additive manufacturing. Additive Manufacturing, 22 (2018), pp. 197-206.

[82] Northcutt, L. A., Orski, S. V., Migler, K. B., & Kotula, A. P. Effect of processing conditions on crystallization kinetics during materials extrusion additive manufacturing. Polymer, 154 (2018), pp. 182-187.

[83] Tseng, J. W., Liu, C. Y., Yen, Y. K., Belkner, J., Bremicker, T., Liu, B. H., ... & Wang, A. B. Screw extrusion-based additive manufacturing of PEEK. Materials & Design, 140 (2018), pp. 209-221.

[84] Valkenaers, H., Vogeler, F., Voet, A., & Kruth, J. P, Screw extrusion based 3D printing, a novel additive manufacturing technology, in COMA'13, (2013).

[85] Pachauri, P., & Hamiuddin, M., Optimization of Injection Moulding Process Parameters in MIM for Impact Toughness of Sintered Parts, International Journal of Advanced Materials and Metallurgical Engineering 1 (2015), pp. 1-11.

[86] Giberti, H., Sbaglia, L., & Silvestri, M. Mechatronic Design for an Extrusion-Based Additive Manufacturing Machine. Machines, 5(4), (2017), 29.

[87] O. Rishi, Feed Rate Effects In Freeform Filament Extrusion: Thesis, Rochester Institute of Technology, (2013).

[88] Fiore, E., Giberti, H., & Sbaglia, L., Dimensional synthesis of a 5-DOF parallel kinematic manipulator for a 3d printer, in 16th International Conference on Research and Education in Mechatronics (REM), (2015).

[89] Giberti, H., Fiore, E., & Sbaglia, L, Kinematic synthesis of a new 3D printing solution, in MATEC Web of Conferences (45) (2016).

[90] Anzalone, Gerald C., Chenlong Zhang, Bas Wijnen, Paul G. Sanders, and Joshua M. Pearce, A low-cost open-source metal 3-D printer, IEEE Access 1 (2013), pp. 803-810.

[91] Giberti, H., Sbaglia, L., & Urgo, M., A path planning algorithm for industrial processes under velocity constraints with an application to additive manufacturing, Journal of Manufacturing Systems, 43 (2017), pp. 160-167.

[92] Monzón, M. D., Gibson, I., Benítez, A. N., Lorenzo, L., Hernandez, P. M., & Marrero, M. D., Process and material behavior modeling for a new design of micro-additive fused deposition, The International Journal of Advanced Manufacturing Technology, 67 (9-12) (2013), pp. 2717-2726.

[93] Oliveira, R.V.B., Soldi, V., Fredel, M.C. & Pires, A.T.N., Ceramic injection molding: influence of specimen dimensions and temperature on solven debinding kinetics, Journal of Materials Processing Technology 160 (2) (2005), pp. 213-220.

[94] Royer, A., Barrière, T., & Gelin, J. C., Development and Characterization of a Metal Injection Molding Bio Sourced Inconel 718 Feedstock Based on Polyhydroxyalkanoates, in Metals, 6(4) (2016).

[95] R. Tandon, Metal injection moulding, in Encyclopedia of Materials: Science and Technolog, Amsterdam, The Netherlands,, Elsevier Science Ltd, (2008), pp. 5439-5442.

[96] V. Boljanovic, Powder metallurgy, in Metal Shaping Processes: Casting and Molding, Particulate Processing, Deformation Processes, Metal Removal, Industrial Press Inc., New York, USA, (2010), pp. 75-106.

[97] Parenti, P., Kuriakose, S., Mussi, V., Strano, M., & Annoni, M., Green-state micromilling of AISI316L feedstock, in World Congress on Micro and Nano Manufacturing (2017).

[98] Parenti, P., Cataldo, S., & Annoni, M. Shape deposition manufacturing of 316L parts via feedstock extrusion and green-state milling, Manufacturing letters, 18 (2018), pp. 6-11.

[99] A. F3091/F3091M-14, Standard Specification for Powder Bed Fusion of Plastic Materials, ASTM International, West Conshohocken, PA, (2014).

[100] A. F3122-14, Standard Guide for Evaluating Mechanical Properties of Metal Materials Made via Additive Manufacturing Processes, ASTM International, West Conshohocken, PA, (2014).

[101] Amir Ghazanfari, Wenbin Li, Ming C. Leu, Gregory E. Hilmas., A novel extrusion-based additive manufacturing process for ceramic parts, in 26th Annual International Solid Freeform Fabrication Symposium, (2016).

[102] Komineas, G., Foteinopoulos, P., Papacharalampopoulos, A., & Stavropoulos, P. Build Time Estimation Models in Thermal Extrusion Additive Manufacturing Processes. Procedia Manufacturing, 21 (2018), pp. 647-654.

[103] Brenken, B., Barocio, E., Favaloro, A., Kunc, V., & Pipes, R. B. Development and validation of extrusion deposition additive manufacturing process simulations. Additive Manufacturing, 25 (2019), pp. 218-226.

[104] Singh, S., Ramakrishna, S., & Singh, R., Material issues in additive manufacturing: A review, Journal of Manufacturing Processes, 25 (2017), pp. 185-200.

[105] Faes M, Valkenaers H, Vogeler F, Vleugels J, Ferraris E., Extrusion-based 3D printing of ceramic components, Procedia CIRP, Volume 28 (2015), pp. 76-81.

[106] K. U. Bletzinger, E. Ramm, Structural optimization and form finding of light weight structures, Computers and Structures 79 (22–25) (2001), pp. 2053–2062.

[107] J. Gonzalez-Gutierrez, D. Godec, R. Guran, M. Spoerk, C. Kukla, C. Holzer, 3D printing conditions determination for feedstock used in fused filament fabrication (FFF) of 17-4PH stainless steel parts, Metalurgija 57 (2018), pp. 117–120.

[108] T. Moritz, U. Partsch, S. Ziesche, U. Scheithauer, M. Ahlhelm, E. Schwarzer, H. Richter, Additive manufacturing of ceramic components, Materials and Processes, Annual Report 2014/15, 28-31

[109] Jafari, M., Han, W., Mohammadi, F., Safari, A., Danforth, S. C., & Langrana, N, A novel system for fused deposition of advanced multiple ceramics, Rapid Prototyping Journal, 6(3) (2000), pp. 161-175.

[110] U. Winkworth Mixer Co., 04 05 2017. [Online]. Available: www.mixer.co.uk/en/product/zx-sigma-mixer-extruder.

[111] Ghazanfari, A., Li, W., Leu, M., Watts, J., & Hilmas, G., Mechanical characterization of parts produced by ceramic on-demand extrusion process, International Journal of Applied Ceramic Technology 14 (3) (2017), pp. 486-494.

[112] Li, W., Ghazanfari, A., McMillen, D., Leu, M. C., Hilmas, G. E., & Watts, J., Fabricating ceramic components with water dissolvable support structures by the ceramic on-demand extrusion process, CIRP Annals-Manufacturing Technology 66 (2017), pp. 225–228.

[113] Gonzalez-Gutierrez, J., Cano, S., Schuschnigg, S., Kukla, C., Sapkota, J., & Holzer, C. Additive Manufacturing of Metallic and Ceramic Components by the Material Extrusion of Highly-Filled Polymers: A Review and Future Perspectives. Materials, 11(5) (2018), pp. 840.

[114] Lieberwirth, C., Harder, A., & Seitz, H. Extrusion based additive manufacturing of metals parts. J. Mech. Eng. Autom, 7 (2017), pp. 79-83.

Figure Captions:

Figure 1: Sintered robocasting scaffolds (a) hydroxyapatite/β-tricalcium phosphate (HA/β-TCP) scaffold with pore size: 330 µm (left) and 150 µm (right) before sintering; (b) corner cross-section obtained by SEM of an HA scaffold (330 µm pore size before sintering) [34]

Figure 2: Schematic diagram of a paste extrusion additive manufacturing system [43]

Figure 3: Example of FDM system used for the extrusion of metal 3D printing filaments [49] with representative products [50]

Figure 4: Machine for extrusion-based AM of metals and ceramics developed at Politecnico di Milano

Figure 5: Process overview for extrusion-based additive manufacturing of metals and ceramics

Figure 6: Type of mixer used for batch mixing (a) Z Sigma Blade Mixer and (b) ZX sigma mixer-extruder [110]

Figure 7: Schematics of extrusion system: (a) Filament based extrusion, (b) Syringe/piston based extrusion, (c) Screw based extrusion [84]

Figure 8: Kinematic machine construction of the extrusion-based system [88]

Figure 9: Green sample printed by this method: (a) overview; (b) the top surface of the green sample (c) cross-section of the green sample [54]

Figure 10: Compressive strength of scaffold varied with different pressure and feeding speed. (a) Compressive strength as a function of air pressure, (b) Compressive strength as a function of feeding speed [38]

Figure 11: Flexural strength and flexural modulus of scaffolds with different vol. % of titanium fibers [35]

Figure 12: Microstructure of a printed alumina sample [101]

Figure 13: Effect of concentration of powder on the stability of scaffolds. (A) Low concentration shows the fiber is deformed. (64 vol% Ti6Al4V powder used.) (B) Optimal concentration (66 vol%). (C) When the powder concentration is high (i.e., 68 vol% Ti6Al4V powder used), there is no adhesion and attachment between the layers [38]

Figure 14: Stress-deformation curve for (a) kaolin with different water content and (b) alumina feedstock with different plasticizer content [68]

Figure 15: Fabrication of a single-wall dental crown [36]

Figure 16: Few examples of application of technology (a) Impeller in green state [101] (b) turbine blower housing after sintering [112] (c) sintered structural parts [107, 114] and (d) square plates [62]

Figure 17: Photograph of a green part and optical micrograph of a sintered multi-material multilayer piezoelectric component transducer [109]

Figures:

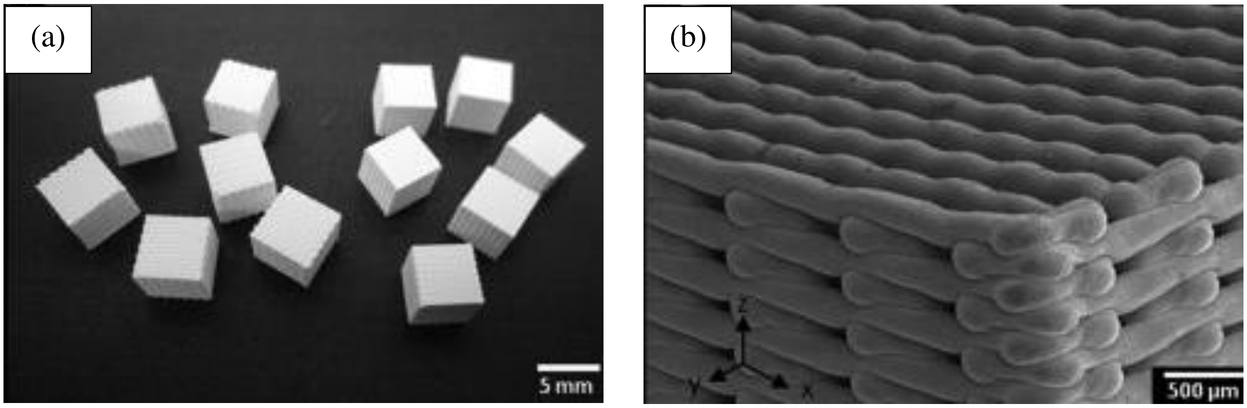

Figure 1

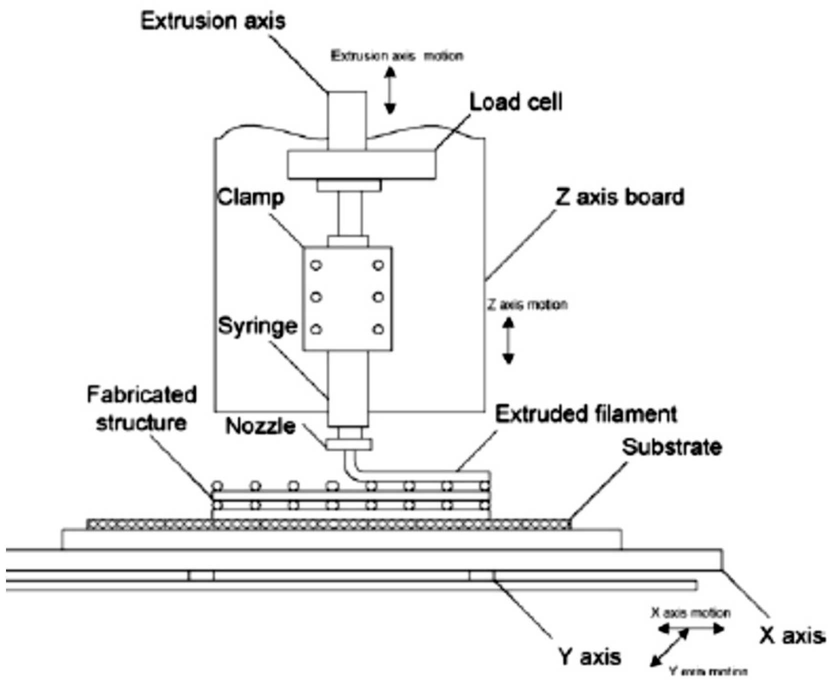

Figure 2

Figure 3

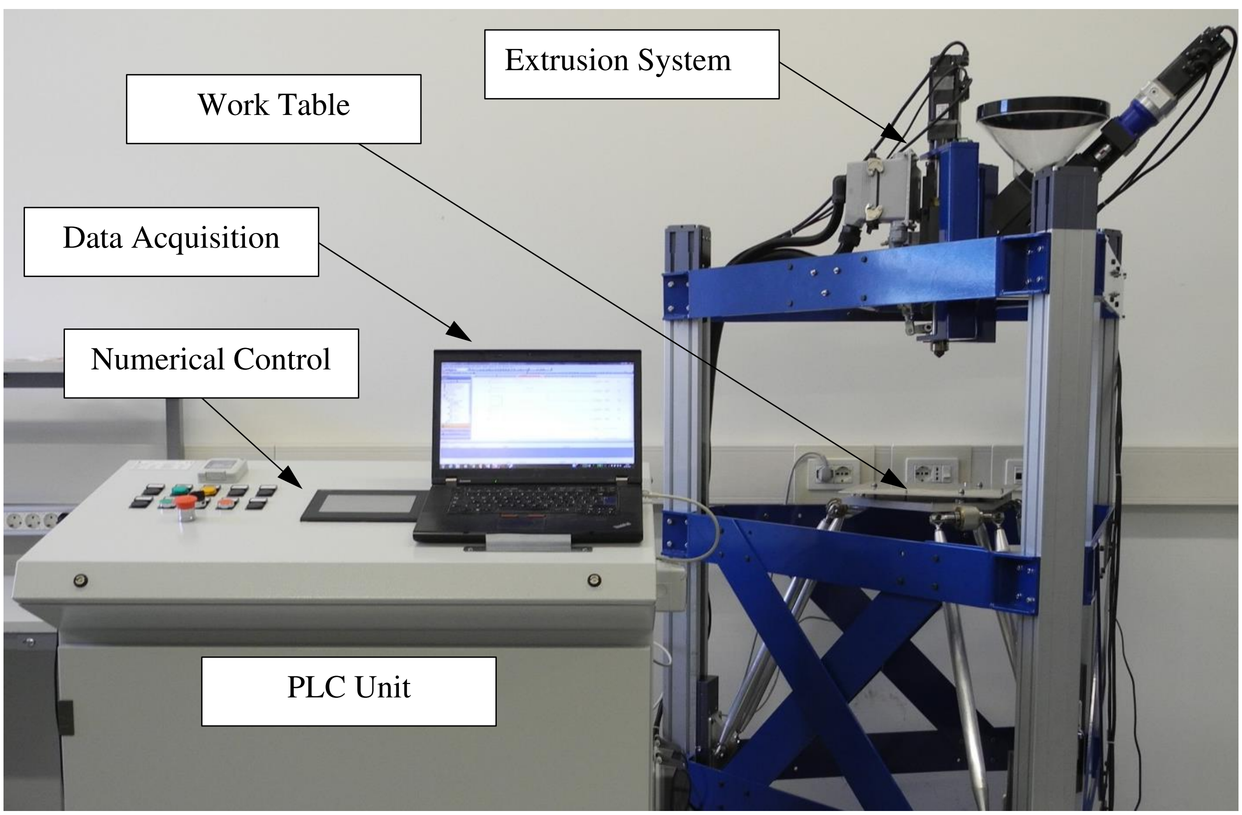

Figure 4

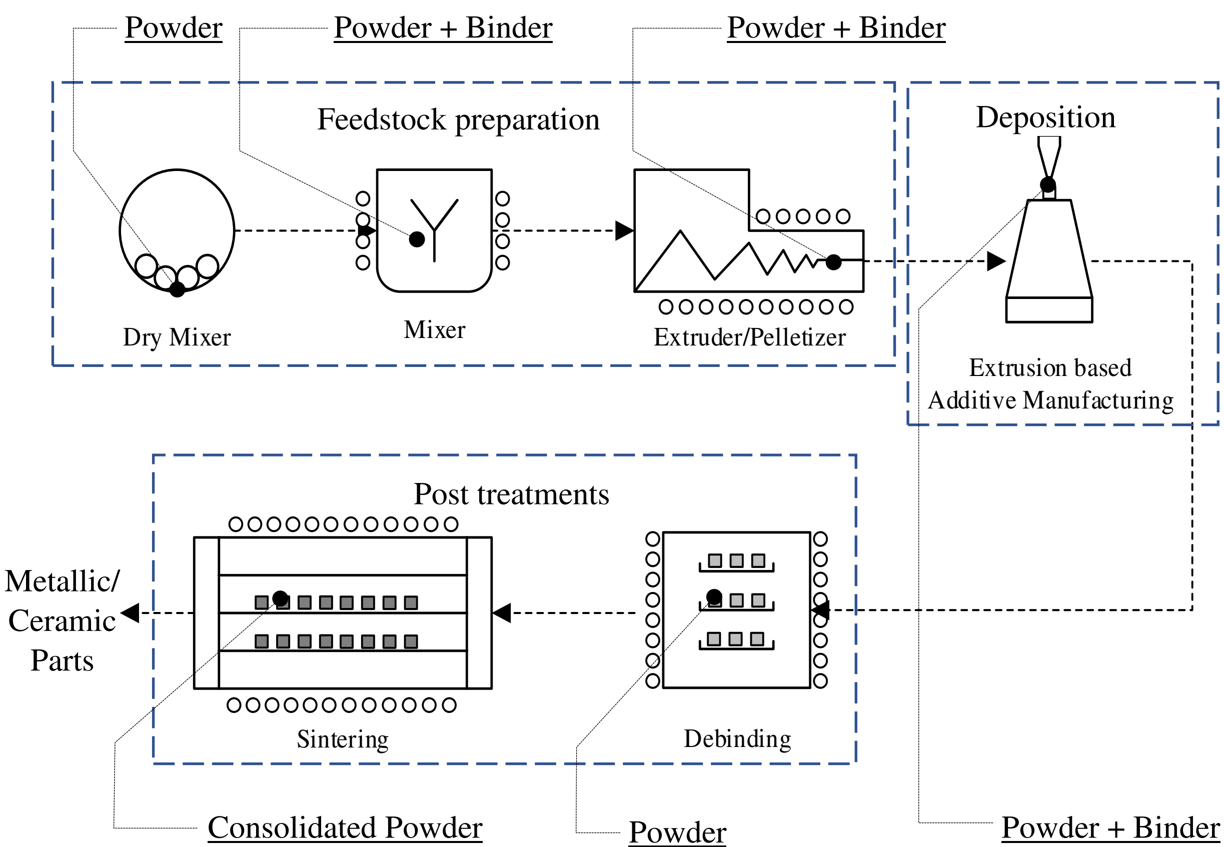
Powder
Powder + Binder
Powder + Binder
Feedstock preparation
Deposition
Dry Mixer
Mixer
Extruder/Pelletizer
Extrusion based
Additive Manufacturing
Post treatments
Metallic/
Ceramic
Parts
Sintering
Debinding
Consolidated Powder
Powder
Powder + Binder

Figure 5

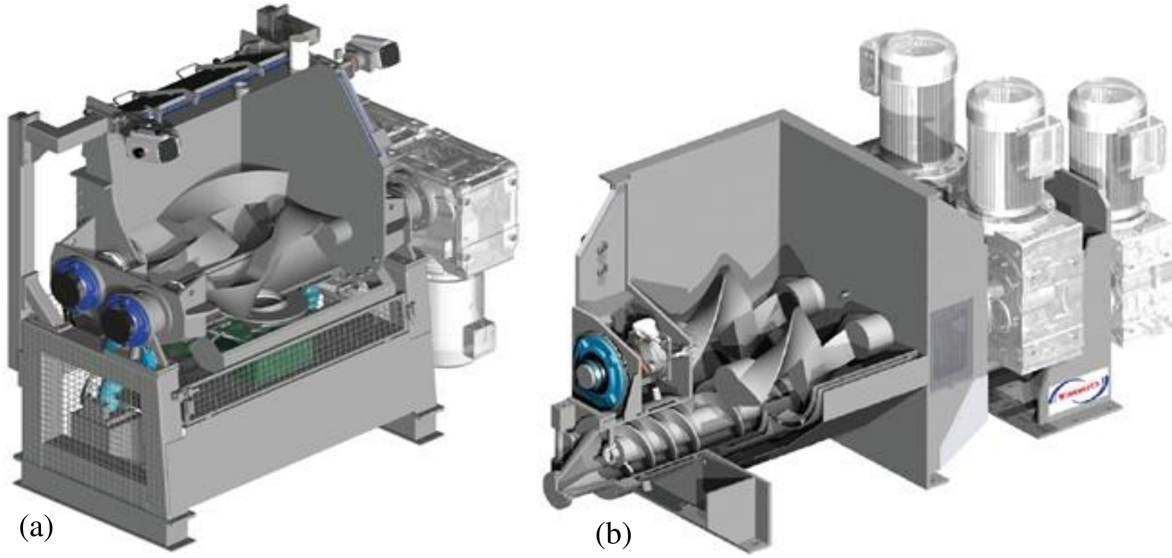

Figure 6

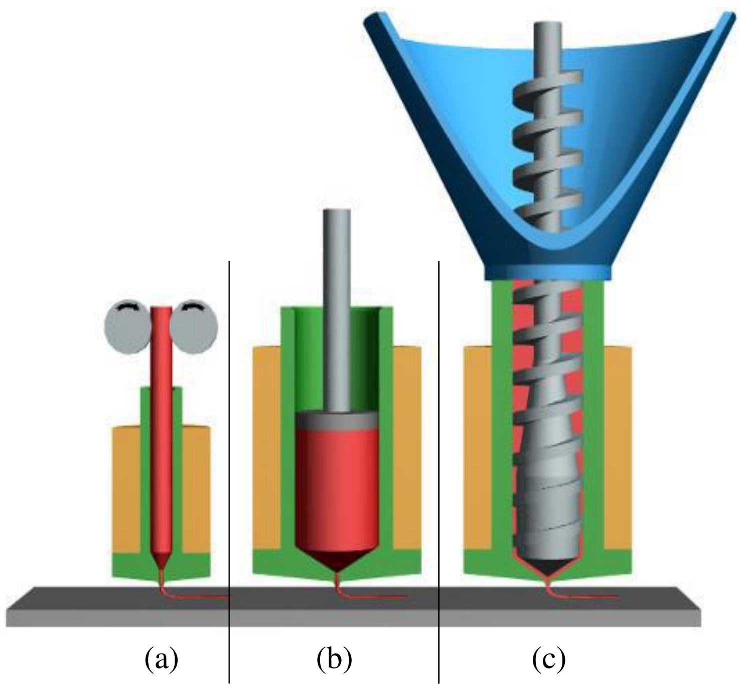

Figure 7

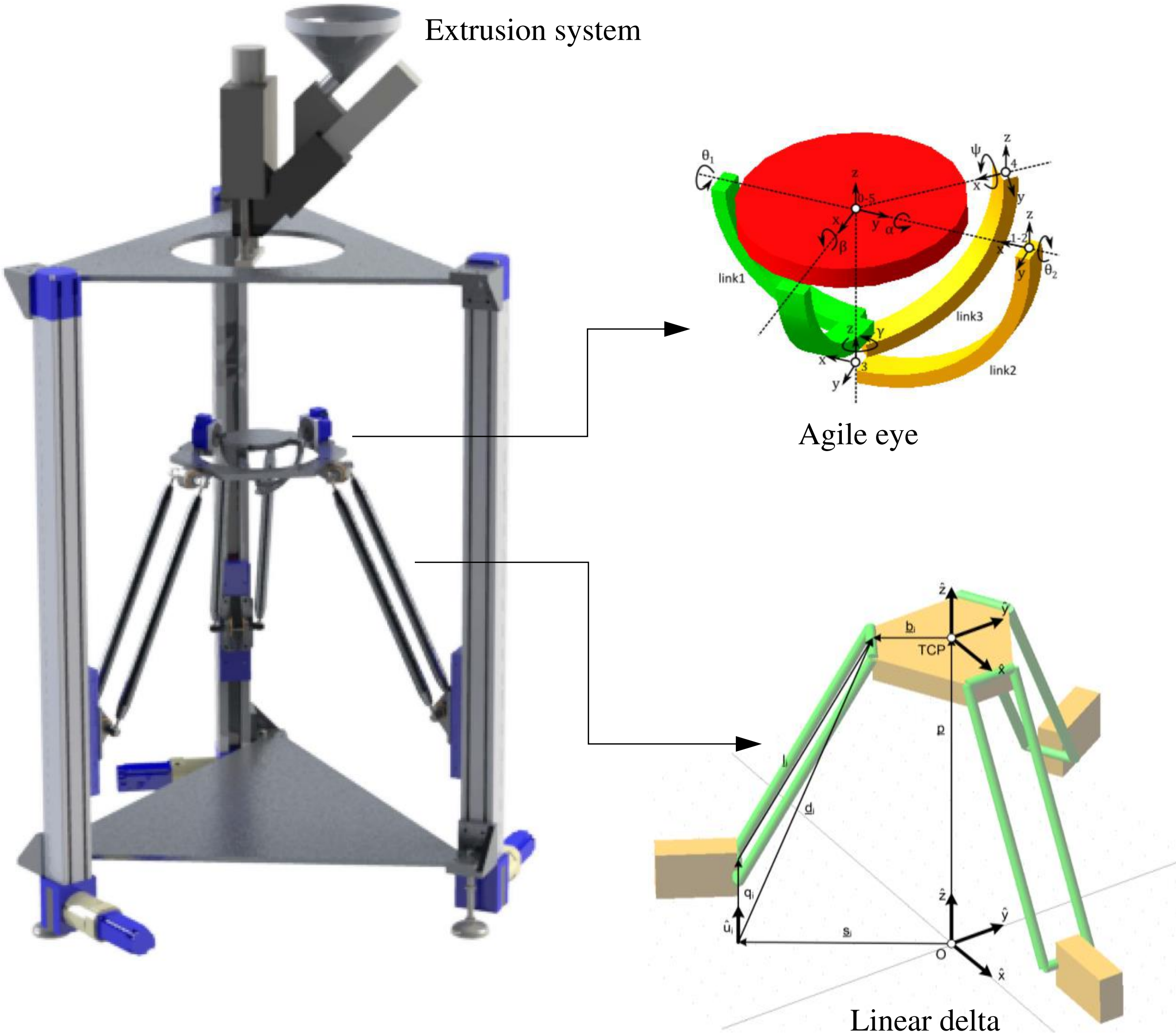
Extrusion system
Agile eye
link1
link2
link3
Linear delta
TCP

Figure 8

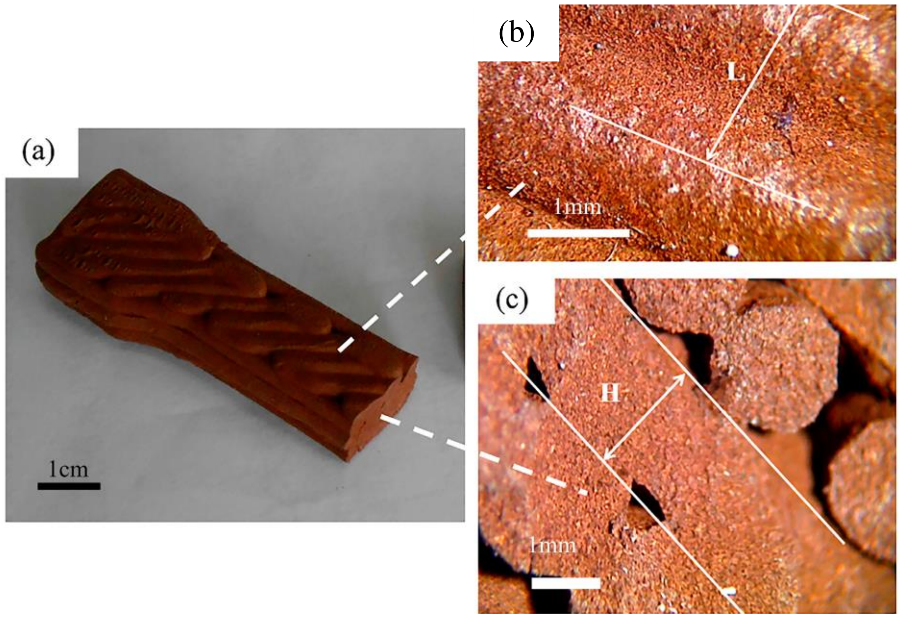

Figure 9

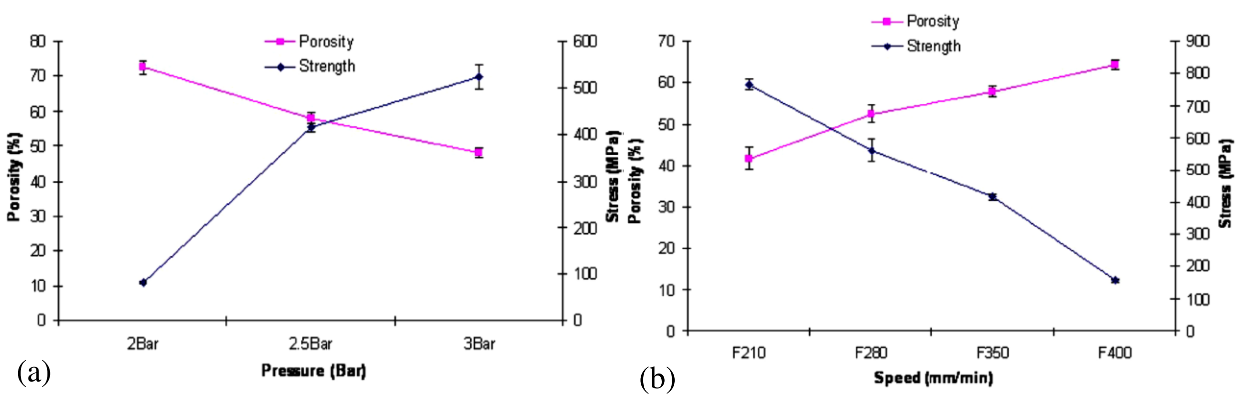

Figure 10

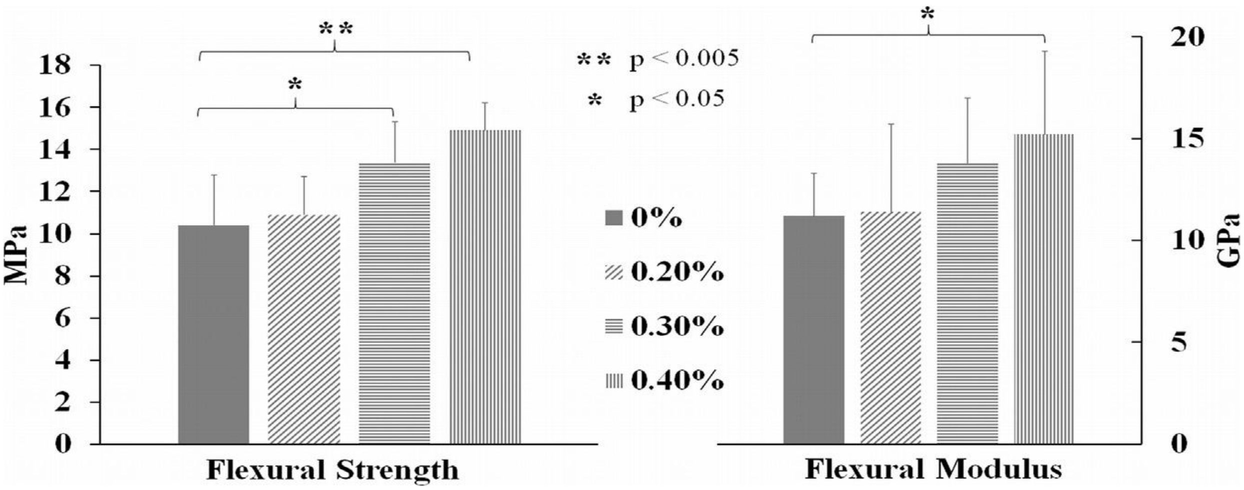

Figure 11

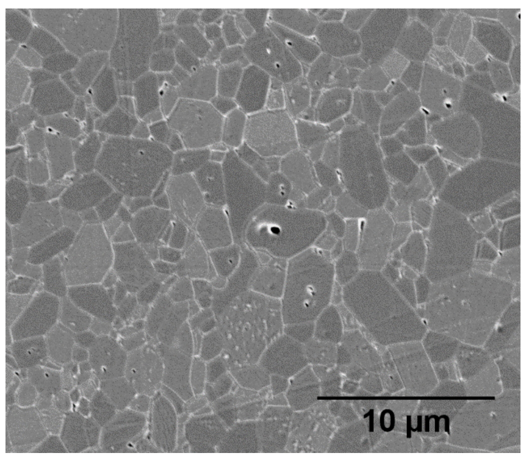

Figure 12

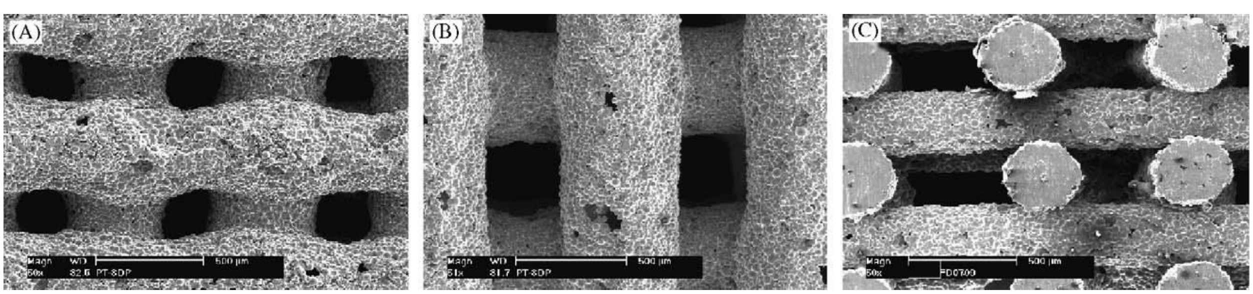

Figure 13

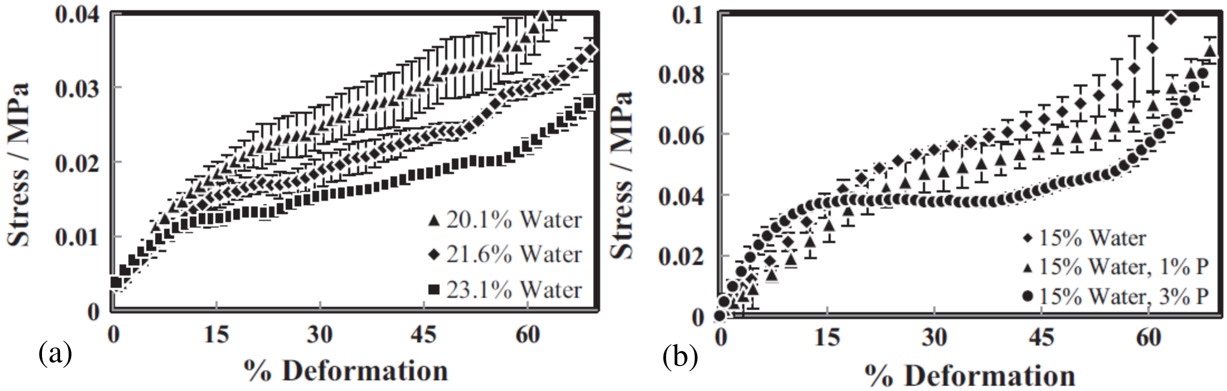

Figure 14

Figure 15

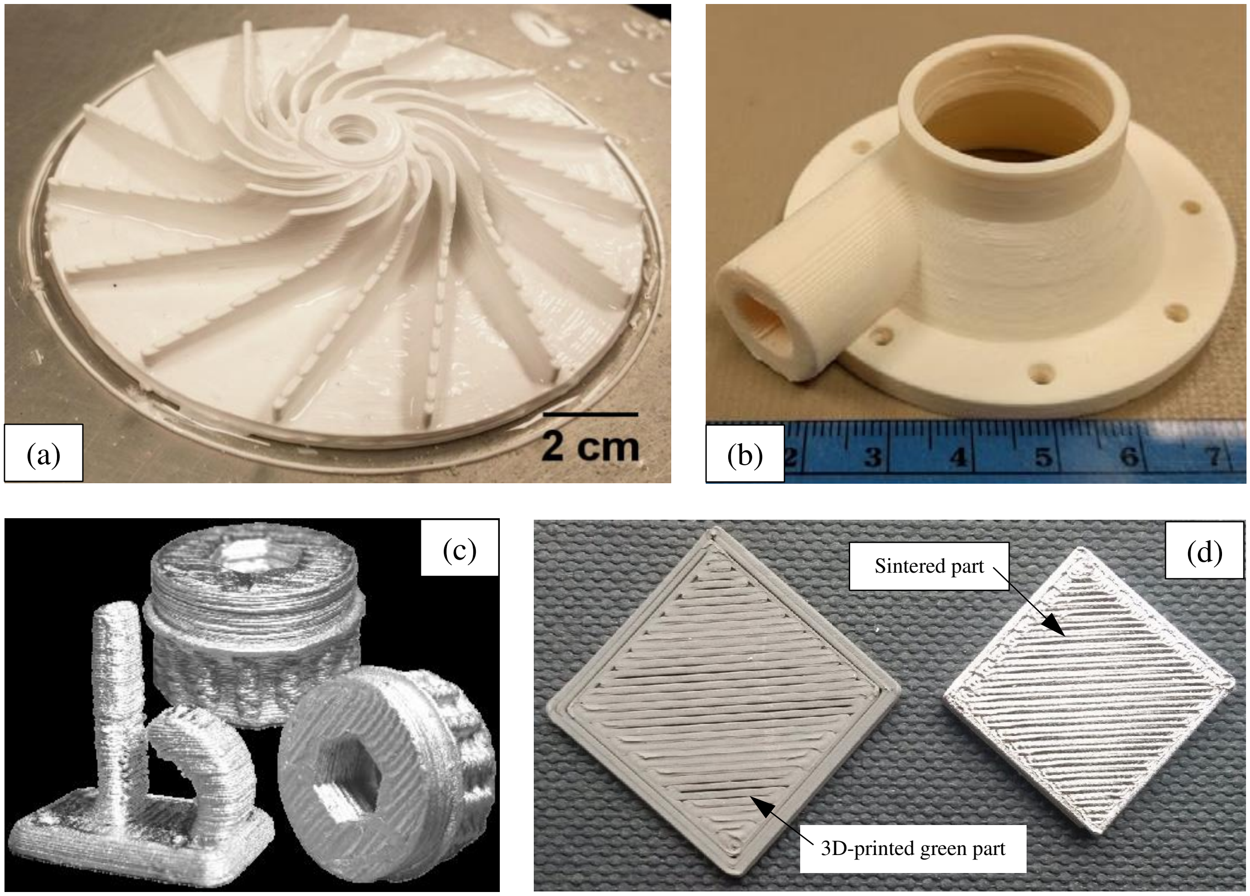

Figure 16

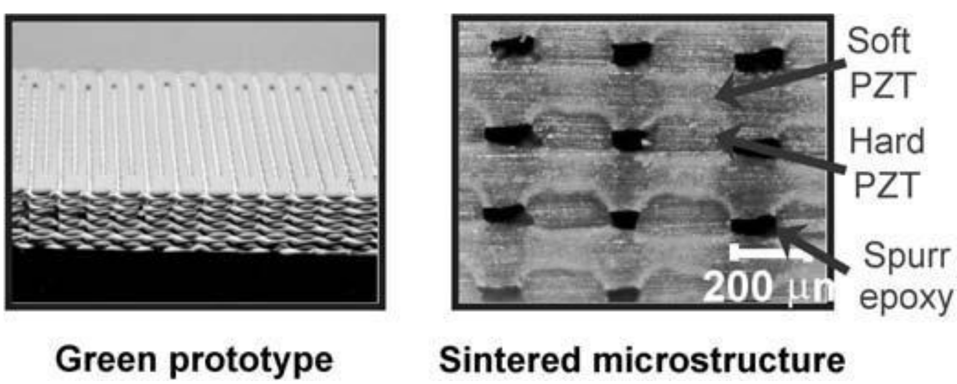

Figure 17

Table captions:

Table 1: Powder-binder systems used in extrusion-based AM of metallic and ceramic parts

Table 2: Feedstock mixtures used in Powder Injection Molding process

Table 3: Properties of copper parts prepared by different additive manufacturing processes [54]

Table 4: Properties of alumina parts prepared by different additive manufacturing processes [111]

Table 5: Characteristics of most of the AM techniques suitable for metals and ceramics

Tables:

Table 1

Powder	Particle size (µm)	Solid Loading	Binder system	Process/ Applications	Reference
Copper	41	65 vol.%	Paraffin wax, LDPE, stearic acid	Extrusion based printing with 2mm nozzle diameter	[54]
Silver	50 nm	83 to 93 wt.%	Poly-4 vinyl phenol	High performance printed transistors	[63]
Ti6Al4V	45	66 vol.%	Methylcellulose and stearic acid	Porous scaffolds	[38]
316L stainless steel	-	60 vol.%	paraffin (PW), high-density polyethylene (HDPE), acetic acid-vinyl acetate copolymer (EVA) and stearic acid (SA)	-	[51]
AISI 630 martensitic stainless steel	13	79 vol. %	Polyethylene glycol (PEG) + other components	-	[53]
High purity alumina	0.32	90 wt.%	PVA + Dolapix CE64	Inkjet 3D printing followed by vacuum infiltration for high density	[64]
5 wt.% yttria doped zirconia	-	88.9 wt.%	Micro-crystalline wax	Bone substitute material and Metal Matrix Composite	[40]
composite (zp150) calcium sulfate	0.6-68.8	-	Commercially formulated 2-pyrrolidone aqueous solution (zb63)	Printed Scaffolds for bone healing	[65]
Barium Titanate	0.85-1.45	-	-	Piezoelectric sensors	[66]
zp150	27	-	Zb63	Printed porous scaffolds	[67]

Tricalcium Phosphate	-	83 wt.%	Stearic Acid, heated paraffin wax	Dental implants	[32]
Alumina Kaolin Red clay	0.8 -9.1	50 vol.%	Paraffin wax, (Dolapix PC67 dispersion agent)	production of cellular ceramic bodies	[68]

Table 2

Powder	Particle size (μm)	Solid Loading	Binder system	Applications	Reference
CP Titanium	-	85 wt. %	Paraffin wax, PP and DBP	-	[69]
Ti-6Al-4V	-	71 vol. %	PW, PEG, PE, SA	Surgical tools	[70]
Ti6Al-4V-4Mo	-	65 vol. %	PW, PP, PMMA, SA	-	[70]
Iron	10	45 vol. %	PP, CW, PW, SA	-	[71]
Carbonyl iron	4.2	63 vol. %	PP, CW, PE, SA	-	[71]
316 L SS (PF-15	8.0	50 vol. %	EVA, CW, PW, SA	-	[71]
430 L SS	10.0	61 vol. %	-	-	[71]
M2 HSS	21.0	60 vol. %	Thermosetting resin	Tools	[72]
Gas atomized copper	10	66.2 vol.%	PE, PW, SA	-	[73]
97%W–2.1%Ni–0.9%Fe (by wt)	16.5	60 vol.%	Paraffin wax–polypropylene mixture	-	[74]
W-Cr	1.8	-	Multi component organic binder	Cutting tools	[75]
Zirconia	-	60 vol. %	Polymers and surfactants	Microparts	[76]
YTZ	0.6	55 vol. %	Paraffin wax–polypropylene mixture	Optical sleeves	[77]
CP alumina	0.6	55 vol.%	PEG, PE wax, SA	-	[78]
alumina–20% zirconia	0.40	57 vol.%	HDPE, PW, SA	-	[79]

Table 3

Process	Density (g/cm^3)	Vickers Hardness (HV)	Yield Strength (MPa)
Wrought Copper	8.90	57	69
Laser additive manufacturing	----	73	----
Electron beam melting	8.84	88	76
Extrusion-based AM	8.15	63	51

Table 4

Process	Relative Density (%)	Hardness (GPa)	Young's modulus (GPa)	Flexural strength (MPa)
Lithography-based ceramic manufacturing	99	----	----	369 to 383
Laser based additive manufacturing	88	----	----	255 ± 17
Robocasting	97	18.6 ± 0.8	----	236 to 248
Freeze-form extrusion fabrication	87 to 92	14.4 ± 0.9	327 ± 20	219
EAM	98	19.8 ± 0.6	371 ± 14	364 ± 50

Table 5

Process	Materials	Resolution (μm)	Advantages	Disadvantages
Robocasting	Metals, ceramic, composites	100 - 450	Fast and economical	Lower resolution and poor properties
EBM	Metals and composites	50 - 100	Fast and suitable for large parts	Poor surface finish and limited materials

SLM	Metals and composites	10 - 50	High accuracy and good strength	Costly and low build up rate
DED/LMD	Metals	50 - 250	High flexibility and no supports required	Material wastage and pollution
Binder-jetting	Metals, ceramics and composites	20 -100	Mass production and economical	Multi-step process
EAM	Metals, ceramics and composites	50 - 100	Economical and good mechanical properties	Multi-step process